The critical spacing factor : preliminary version

Fagerlund, Göran

1993

LUND INSTITUTE OF TECHNOLOGY
Division of Building Materials

THE CRITICAL SPACING FACTOR

Preliminary version

A contribution to the BRITE/EURAM project
BREU-CT92-0591
"The Residual Service Life of Concrete Structures"

Göran Fagerlund

Report TVBM-7058
Lund , October 1993

Content

		Page
Preface		1
1 Summary		2
2 Frost destruction mechanisms		3
2.1	Freezable water	3
2.2	Damage mechanism 1; Freezing of a closed container	6
2.3	Damage mechanism 2; Hydraulic pressure	11
2.4	Damage mechanism 3; Microscopic ice lens growth	17
2.5	Damage mechanism 4; Macroscopic ice lens growth	22
3 The critical fictitious spacing factor		25
3.1	Definition	25
3.2	Experimental technique	26
3.3	The critical fictitiuos spacing factor at salt scaling	28
3.3.1	Main study; many variables in mix design and compaction	28
3.3.2	Special study 1; effect of the air content	32
3.3.3	Special study 2; effect of the cement type	33
3.3.4	Special study 3; effect of the type of air-entraining agent	36
3.3.5	Studies published by other authors38	
3.4	The critical fictitious spacing factor at freezing in pure water	39
4 The critical true spacing factor		40
4.1	Definition; method of determination	40
4.2	The critical true spacing factor at salt scaling	41
4.3	The critical true spacing factor at freezing in pure water	43
4.3.1	Main study	43
4.3.2	Special study 2; effect of the cement type	46
4.3.3	Direct determination of the critical size	48
Literature		49

Preface

This report is produced within the BRITE/EURAM project BREU-CT92-0591 "The Residual Service Life of Concrete Structures".

Six partners are involved in the project:

1: British Cement Association (The Coordinator)
2: Instituto Eduardo Torroja, Spain
3: Geocisa, Sopain
4: The Swedish Cement and Concrete Research Institute
5: Cementa AB, Sweden
6: Div. of Building Materials, Lund Institute of Technology , Sweden

Three deterioration mechanisms are treated in the project:
1: Corrosion of reinforcement
2: Freeze-thaw effects
3: Alkali-silica reaction

This report refers to Task 4: "Assessment of deterioration rates".

Lund, 12 October, 1993

Göran Fagerlund

1. Summary

Different frost destruction mechanisms are treated. It is shown theoretically that so-called critical sizes exist. They can be defined as the biggest piece of a cement paste that can be completely water saturated during a freezing test without suffering any damage. It is also shown that the critical size is different for different specimen geometries. One can talk about a critical thickness, a critical sphere or a critical shell thickness which is normally also called a critical spacing factor. There are simple geometrical relations between the different critical sizes; if one is known, the other can be calculated. The critical thickness and the critical sphere are true material properties while the critical spacing factor also to a certain degree depends on the air pore structure. Despite this, the spacing factor is more widely used than the other parameters.

The normal way of defining the critical spacing factor is to assume that all air pores are air-filled also during a practical freeze-test. This gives a **fictitious spacing factor**. Results from a large number of tests for determination of the critical fictitious spacing factor with regard to salt scaling are presented. It has not been possible to find a very well-defined value. The value depends to some degree on the lowest temperature used in the test. It seems, however, as if a value of 0,16 mm is on the safe side although there are results indicating that a value of 0,10 mm is necessary for some concretes while 0,25 mm is sufficient for other concretes. It is quite evident that the fictitious spacing factor is not perfect for estimating salt scaling resistance. For freezing in pure water it seems as if the critical fictitious spacing factor is about 0,22 to 0,25 mm.

In reality, a certain fraction of the air pores are water-filled during the test. This means that **the true spacing factor** during a test is always considerably bigger than the fictitious. Consequently, also the critical true spacing factor is bigger than the fictitious. The critical true spacing factor can be determined from the so-called critical degree of saturation of a concrete assuming the air pore distribution is known. Some results for freezing in pure water are presented. The order of size is 0,30 to 0,35 mm for freezing in pure water. Another possibility is to freeze-test completely water saturated cement pastes and measure the size of the fragments. For pre-dried and resaturated pastes this gives the value 0,40 mm for freezing in pure water and 0,54 mm for freezing in 3% NaCl-solution.

2. Frost destruction mechanisms

2.1.Freezable water

The freezing-point of water in a pore is lower the smaller the pore diameter.The exact relation between the pore size and the freezing point is not fully clarified. It depends on which types of meniscus systems ice-water, ice-vapour and water-vapour that appear in the entire complex pore system; Defay et al /1966/. A reasonable assumption is that the ice phase remains under ordinary atmospheric pressure while the unfrozen part of the pore water is exposed to an under-pressure that is described by the Kelvin law of capillary condensation. This implies that the interfaces between ice and vapour are plane while the interfaces between water and vapour are curved in the normal manner. No curved interfaces between ice and water are assumed to appear. Besides, water that is adsorbed on the pore walls is supposed to be unfreezable. Under these assumptions the following realation between the pore diameter and the freezing temperature is valid. See Fagerlund /1973/.

$$r = -\frac{2\cdot\sigma_{lg}\cdot M}{\rho_l\cdot\Delta H}\cdot\frac{1}{\ln\{(T_o-\Delta T)/T_o\}} + 19{,}7\cdot10^{-10}\,(1/\Delta T)^{1/3} \qquad (1)$$

Where,

r	the pore radius (m)
σ_{lg}	the surface tension between water and vapour (N/m)
M	the molecular weight of water (kg/mole)
ρ_l	the density of water (kg/m^3)
T_o	the freezing point of bulk water (273,15°K)
ΔT	the freezing point depression (°K)
ΔH	the molar heat of fusion of water (J/mole)

Where the first term on the right hand side is the radius of the liquid meniscus or ice body and the second term is the thickness of the adsorbed layer. In Table 1 some examples of the relation between the pore diameter and the freezing point are shown. The corresponding relative humidity (RH) according to the Kelvin equation is also listed in the table.

Therefore, at normal freezing temperatures neither the water in the gel pores nor the water in the finest capillaries is freezable. Some measurements of the freezable water in concrete at -15°C are shown in Fig 1. Curve A shows the results for concretes that have been stored in water all the time from the mixing to the test. Curve B shows the results for companion specimens that have been predried once at +105°C and then resaturated be means of vacuum treatment. The total evaporable water content is also shown in the figure.

The freezable water content is always lower than the total water content. For a never-dried concrete it seems as if there is no freezable water at all if the water-cement ratio is below 0,3. For a pre-dried concrete, however, the freezable

water content is much higher. So for example, for a pre-dried concrete with W/C=0,3 the freezable water is almost as high as for a never-dried concrete with W/C=0,6. Similar effects have also been found by Sellevold et al /1982/. There are also indications that similar effects occur even when the concrete has been exposed to much milder drying at room temperature; Fagerlund & Modéer /1974/.

Table 1: Relation between the pore diameter, the corresponing relative humidity when capillary condensation takes place in the pore and the freezing point.

Diameter (Å)	RH (%)	Freezing point (°C)
450	95	-6
280	92	-10
200	88	-15
160	85	-20
115	80	-30
95	76	-40

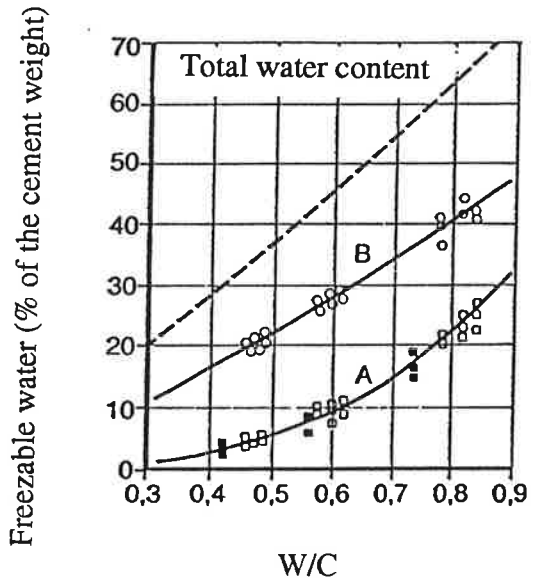

Fig 1: Freezable water of concrete at -15°C. A: Never dried specimens. B: pre-dried and resaturated specimens. Vuorinen /1973/.

The reason for this change in the freezable water caused by drying has never been fully clarified. It ought to depend on some sort of structural change brought about by drying. The most plausible explanation is that a very large fraction of the potentially freezable water in the never-dried concrete is located in isolated small capillary pores. This water remains unfrozen -supercooled-

until it freezes by homogeneous nucleation at about -40°C. The supercooling of water increases with decreasing size of the water volume. The average freezing point of 1mm water drops is about -24°C. For 0,01 mm drops it is about -40°C; Bigg /1953/. Below this temperature supercooling cannot occur. Large ice formation at this temperature level has often been observed in calorimeter experiments with never-dried cement paste; see Fig 2. This large ice formation might depend on the homoneous freezing of supercooled water in numerous isolated capillaries and not on real freezing point depression in a large number of pores with the diameter 95 Å which corresponds to -40°C (Table 1).

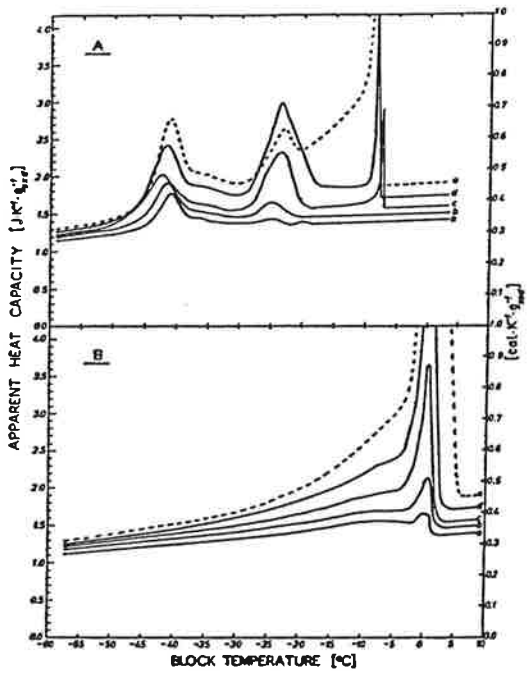

Fig 2: Calorimetric measurements of never dried cement pastes. A: Cooling phase. B: Warming phase. Bager & Sellevold /1983/. (a. W/C=0,35; b. W/C=0,40; c. W/C=0,45; d. W/C=0,50; e. W/C=0,60)

At the pre-drying, a microcrack system might develop in the cement gel surrounding the previously isolated capillaries. Thereby, ice-formation can be initiated by ice from other, coarser pores penetrating the crack system. Therefore, ice-formation in the pre-dried specimen occurs at almost the correct temperature determined by the actual pore size. The correctness of this explanation based on supercooling is strengthened by the fact that ice melting in never-dried specimens occurrs at considerably higher temperatures than ice formation; see Fig 2. Such a hysteresis between ice melting and ice formation should appear if supercooling phenomenons af the type discussed appears. The hysteresis betwen ice formation and ice melting is also considerably smaller for pre-dried specimens.

For a concrete under practical conditions at lowest imaginable temperature one can roughly assume that all capillary pores contain freezable water while the gel pore water is unfrozen. This implies that the maximum freezable water content is; Powers & Brownyard /1948/:

$$w_f = B(W/B - 0{,}39 \cdot \beta) \qquad (2)$$

Where

w_f	the freezable water (litres/ m^3)
B	the binder content (kg/m^3)
W	the mixing water content ($litres/m^3$)
β	the degree of hydration (1)

The equation is strictly speaking only valid for concrete with portland cement but can also be used for an approximative estimate of the freezable water in concretes with mineral admixtures.

The non-freezable water is further on epressed in terms of a fraction k_θ of the total evaporable water content. If it is assumed that only the gel pores and the capillary pores contain water the following relation is valid; Powers&Brownyard /1948/.

$$1 - k_\theta = (W/B - 0{,}39 \cdot \beta)/(W/B - 0{,}19 \cdot \beta) \qquad (3)$$

For some typical concretes the values in Table 2 are valid:

Table 2: The maximum amount of freezable water in some typical concretes

W/B	B (kg/m^3)	β	w_f ($litres/m^3$)	w_f/B	k_θ
0,75	240	0,80	105	0,44	0,27
0,65	275	0,80	93	0,34	0,32
0,55	330	0,75	85	0,26	0,37
0,45	400	0,70	70	0,18	0,45
0,30	500	0,50	50	0,10	0,51

The agreement between these values and the experimental in Fig 1 is good. For the highest W/B-ratio the theoretical value is, however, somewhat higher.

2.2 Damage mechanism 1; Freezing of a closed container

In the simpliest case every small "unit cell" of the concrete can be looked upon as a closed container. No water transfer is possible from the the place where ice is formed. The reason might be that the concrete does not contain any air-filled space or that the permeability of the pore wall is so low that water is practically immobilized. The 9% volume increase when water is transformed to ice must therefore be taken care of in the neighbourhood of the freezing site; i.e. within the "local container". Very high pressures might develop if the container is

completely water-filled. The phase diagram ice-water shows that a pressure of 10MPa is needed to lower the freezing point by 1 °C. Therefore, at -20°C a pressure of about 200 MPa is needed if ice formation shall be prevented. Two simple models can be used for estimating the maximum pressures in the water saturated concrete; see Fig 3. In both models the cement paste phase is supposed to be a waterfilled and incompressible hole-sphere of unit volume (1 m^3).

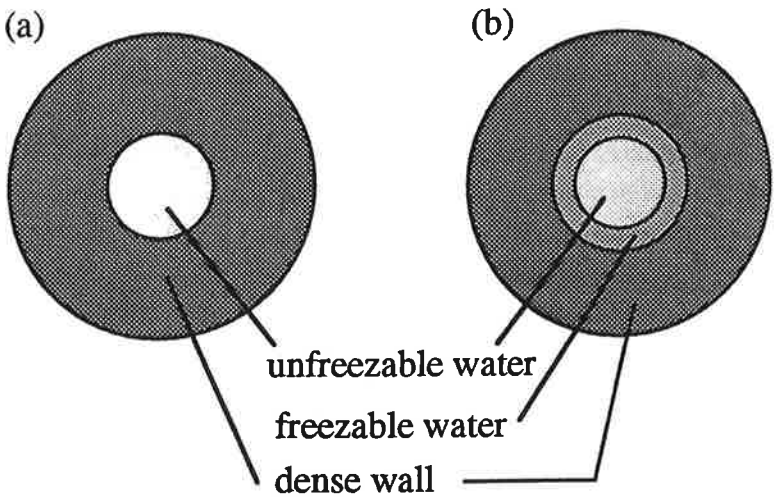

Fig 3: Illustration of damage mechanism 1; hole-sphere with impermeable wall. (a) Only freezable water in the hole. (b) All evaporable water in the hole.

Model 1: All potentially freezable water is located in the hole while all non-freezable water is located in the sphere-wall; Fig 3a. The container wall is supposed to be impemeable and no pressure from the water in the hole is supposed to be transferred by hydraulic action to the water in the wall. Then the maximum tangential stress in the wall due to an inner pressure along the periphery of the hole is; Timoshenko & Goodier /1951/:

$$\sigma_t = p(0{,}5+W_f)/(1-W_f) \qquad (4)$$

Where

σ_t	the tangential sress in the container wall (MPa)
p	the inner pressure (MPa)
W_f	the total freezable water (m^3/m^3)

The pressure p does only depend on the temperature since no volume expansion is supposed to take place. As said above $p \approx 10 \cdot \Delta\theta$ where $\Delta\theta$ is the freezing point depression due to internal pressure in the water. Therefore:

$$\sigma_t \approx 10 \cdot \Delta\theta(0{,}5+W_f)/(1-W_f) \qquad (5)$$

The tensile strength of a cement paste is hardly above 10 MPa. This means that according to eq (5) a cement paste cannot resist freezing to a temperature that is

lower than about -2°C even if the freezable water is as low as 1% of the cement paste volume or 0,3 % of the concrete volume. For a typical concrete with W/C=0,6 the freezable water is about 90 litres per m^3 or 9% of the concrete volume; see Table 2. This corresponds to about 30 % of the cement paste volume. Such a concrete can according to eq (5) only resist freezing to about -0.9°C.

Model 2: All pore water is supposed to be contained in the hole and all solid material in the wall. The maximum stress is given by eq (5) with W_f exchanged for the total cement paste porosity P. This model is physically more reasonable than Model 1 and gives even smaller freezing point depressions. The porosity of a cement paste with W/C=0,6 is about 50%. This means that the maximum freezing point depression is only about 0,5°C.

The calculations clearly show that a completely water saturated concrete cannot resist freezing without damage. Even a very low water content is enough to damage the concrete seriously. Therefore, the concrete must contain a certain amount of air-filled space. One can make an estimate of the maximum allowable effective degree of saturation of the concrete by neglecting the compressibility of water and ice and assuming that fracture occurrs when the 9% volume expansion of water corresponds exactly to the relative volume ductility of the container. These assumptions leads to the following relation:

$$S_{eff,CR} = 0{,}917 + 3\cdot\varepsilon_b(1-2\nu)/[1.09\cdot P(1-k_\theta)] \qquad (6)$$

Where

S_{eff}	the effective degree of saturation defined by eq (7)
ε_b	the relative linear ductility (m/m)
ν	Poisson´s ratio
P	the total porosity (m^3/m^3)
k_θ	the non-freezable water as fraction of the total porosity P (m^3/m^3)

k_θ is a function of the freezing temperature; the lower the temperature the lower the value of k_θ. In the following, the lowest value of k_θ in the practical case is used; i.e when the temperature is about -30°C.

The second term on the right hand side expresses the effect of the ductility of the specimen. For a completely stiff material $S_{eff,CR}$ is always 0,917.

S_{eff} is defined

$$S_{eff} = W_f/(W_f+a) = 1 - (a/P)/(1-k_\theta) \qquad (7)$$

Where a (m^3/m^3) is the air-filled pore volume as a fraction of the entire concrete volume. The following approximative values can be used; ν=0,20; ε_b=0,2‰. Then eq (6) can be written:

$$S_{eff,CR} = 0{,}917 + 3{,}3\cdot10^{-4}/[P(1-k_\theta)] \qquad (8)$$

This equation can be used for a calculation of the absolute maximum amount of freezable water in a completely saturated concrete as well as the the absolute minimum volume of air-filled pores. This will be shown by two examples.

Example 1: Even in an extremely dense concrete with W/C=0,3 the total porosity P is about 10%. Then, by eq (8) it is found that the maximum allowable freezable water which is expressed by the parameter $(1-k_\theta)$ is 0,04 m^3/m^3. The maximum amount of freezable water therefore is $0,04 \cdot P = 0,004$ m^3/m^3 or 4 litres per m^3 of concrete. This means that very little freezable water is sufficient to damage the specimen when this is completely saturated.

Example 2: A porous outdoor concrete with the W/C-ratio 0,7 and the porosity15% is regarded. According to Table 2 the freezable water is about 100 litres/m^3 and the factor k_θ is about 0,30. According to eq (8) the maximum value of $S_{eff,\,CR}$ =0,920. According to eq (7) the minimum air content therefore is about 0,9% or 9 litres per m^3 of concrete. This example shows that a very small air content is sufficient to protect the concrete under the assumption that this air volume is located directly at the freezing site. As will be shown below, in the practical case, water has to move a rather long distance before it can be taken care of in an air filled pore. This flow creates stresses. The consequence of this is that the real air content that is needed is much higher than the theoretical minimum just calculated.

The damage mechanism 1 can be applied to at least five cases:

Case1: The absolute minimum air content in a concrete. This application has just been shown by example 2.

Case 2: The effect of porous aggregate grains embedded in the concrete. Such grains can in a first approximation be regarded as closed containers from which water transfer to the cement paste is impossible. Aggregate grains having a total porosity above 0,5 to 1% and becoming waterfilled when embedded in the paste to an effective degree of saturation higher than 0,92 must, according to the theoretical analysis performed, be very dangerous. This has also been found in practice; see Fig 4. Only aggregate pores smaller than about 1 μm become water-filled when the aggregate is sealed by the paste. Therefore, fine-porous natural aggregates such as limestone and slate are exceedingly frost sensitive. Theoretical analyses of the stress conditions in the embedded aggregate and in the surrounding cement paste during freezing has been performed in Fagerlund /1978/.

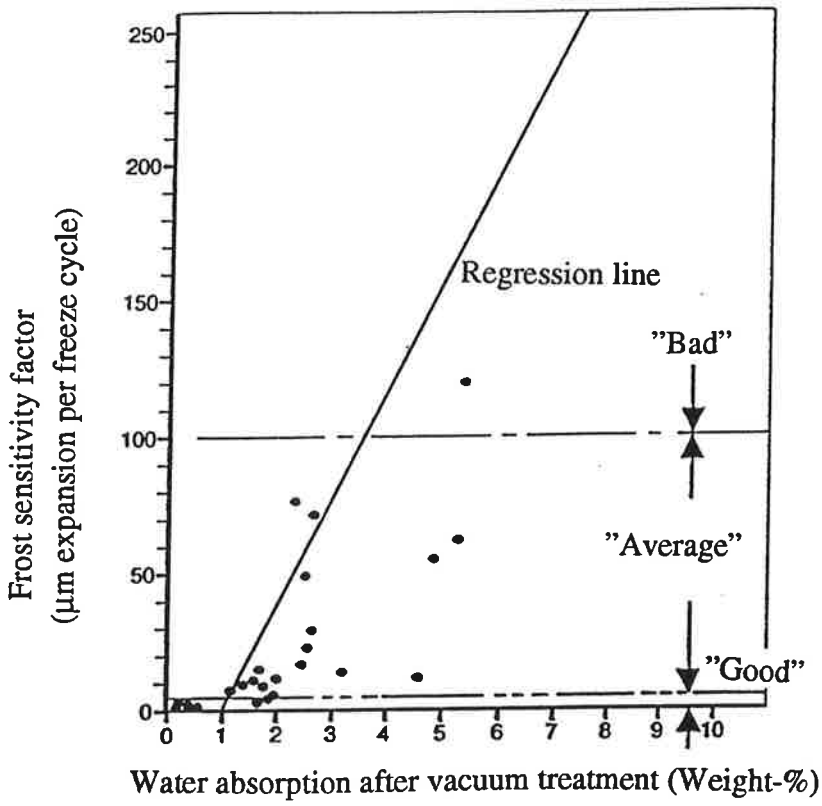

Fig 4: Expansion at freezing of concrete as function of the porosity of the aggregate. Larson & Cady /1969/.

3: High performance concrete with very low W/C-ratio. It is sometimes claimed that one can avoid air in such a concrete due to its low amount of freezable water or even lack of any freezable water. The calculations show however that also a very low amount of freezable water (about 5 litres per m^3) is sufficient to destroy the concrete if it can become fully saturated. Therefore, a certain but often low air content is required even in a very dense concrete.

4: Freezing of young concrete. Already Powers /1962/ showed by a theoretical/empirical analysis that the closed container mechanism could be applied to this case. This was verified purely theoretically by Fagerlund /1980/, /1993/. The self-desiccation occurring as a consequence of cement hydration creates local air-filled pores distributed over the entire cement paste volume. Damage can no longer occur when the self desiccation is so high that the effective degree of saturation fall below 0,917. Then, the volume expansion due to ice formation can be taken care of locally at each individual capillary. Fagerlund /1993/ shows theoretically that the required degree of hydration for protecting the paste is $\beta=0{,}55 \cdot W/C$. This relation is exactly the same as the half empirical relation derived by Powers/1962/ and almost the same as the purely empirical relation found by Jung /1967/; $\beta=0{,}48 \cdot W/C$.

5: Cracks. Cracks that are open to the surface of the concrete can be assumed to be water-filled during very wet conditions. The stresses occurring as a conse-

quence of freezing depend on the crack geometry, on the crack frequency and on the possibility of water to be squeezed out from the crack during freezing. The worst case occurs when the crack is so deep that water cannot be squeezed out at the same time as water transfer into the cement paste matrix is impossible. Then, very high pressures can probably appear. Normally, however, the cement paste contains some air-filled pores to which the surplus water can be displaced. It is possible to make a simplified calculation of the maximum tolerable crack width by the following equation. It is based on the assumption that the air content in a cement paste slice of a certiain critical thickness $D_{CR}/2$ shall be high enough to accomodate displaced water from half the crack and from the cement paste slice itself. D_{CR} is the so called critical thickness which will be described in the next paragraph. If 1 m^2 of crack surface is regarded the following relation is valid:

$$0{,}09 \cdot t_{max}/2 + 0{,}09 \cdot W_f \cdot D_{CR}/2 = a \cdot D_{CR}/2 \qquad (9)$$

Where

t_{max}	the critical crack width (m)
W_f	the freezable water in the cement paste (m^3/m^3)
D_{CR}	the critical thickness (m)
a	the air content in the cement paste (m^3/m^3)

The equation can be simplified to:

$$t_{max} = D_{CR}\,(a - 0{,}09 \cdot W_f)/0{,}09 \qquad (10)$$

Let us assume that D_{CR}=1mm (see below) and W_f=200 litres per m^3 of cement paste. Then the following maximum allowable crack widths are valid:

* air content 6% (2% in concrete); t_{max}=0,46 mm
* air content 12% (4% in concrete); t_{max}=1,1 mm
* air content 18% (6% in concrete); t_{max}=1,8 mm

2.3 Damage mechanism 2; Hydraulic Pressure

It is known by experience that more air is needed in a concrete than that predicted by damage mechanism 1. In many cases much more air is needed. One reason described by damage mechanism 2 is that excess water caused by freezing cannot be accomodated at the freezing site but has to expelled to an air-filled pore which is big enough to take care of it without causing stresses. This water transfer occurs through a narrow and partly ice-filled web of capillary pores and gel pores. High pressure can therefore arise and be transferred to the pore walls as tensile stresses. The pressure is often referred to as hydraulic pressure. The concrete is damaged when the tensile stresses exceed the tensile strength. The damage mechanism is visualized in Fig 5.

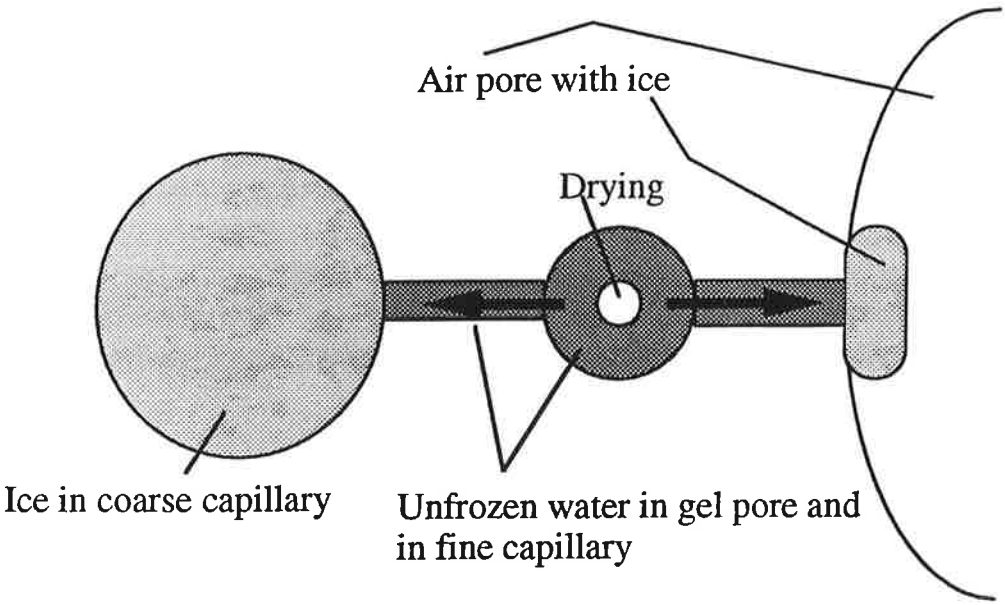

Fig 5: Illustration of damage mechanism 2.

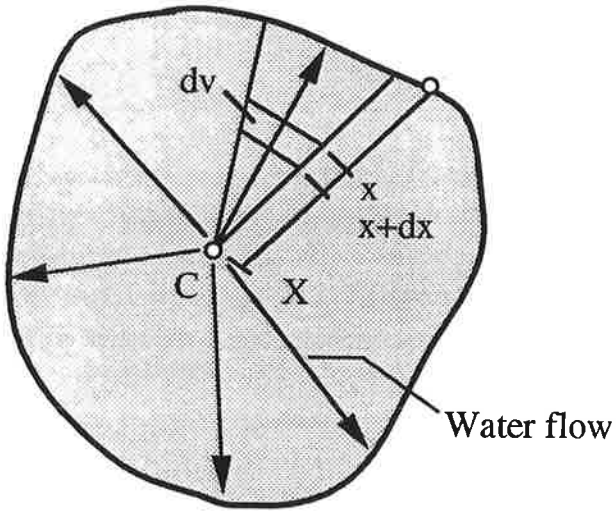

Fig 6: Model for calculating the critical size. Fagerlund /1986/.

The hydraulic pressure can be calculated for some simple geometries. Fig 6 shows a completely water saturated materials volume exposed to freezing. Water is transferred from a central point C flowing towards the periphery. The water pressure can be described by Darcy´s law. The following expression is valid for the pressure p(x) in the marked material sector at the distance x from the periphery; Fagerlund /1986/.

$$p(x) = 0{,}09\cdot(dW_f/dt)\cdot(1/K)\cdot\int_0^x [v(x)/a(x)]\cdot dx \qquad (11)$$

Where

dW_f/dt the rate of ice formation [$m^3/(m^3\cdot s)$]

K the permeability [$m^2/(Pa\cdot s)$]

a(x) the cross section of the water flow at coordinate x (m^2)

v(x) is defined:

$$v(x) = \int_x^X dv \qquad (12)$$

Where dv is the size of the volume element $a(x)\cdot dx$. v(x) therefore is the total sector volume between the coordinate x and the point C which is the origin of the water flow.

The integral in eq (11) evidently is a function of the geometry of the specimen. The maximum pressure p_{max} is occurring in the point C. Then eq (11) can be formulated:

$$p_{max} = 0{,}09\cdot(dW_f/dt)\cdot(1/K)\cdot f(X) \qquad (13)$$

Where the function f(X) is a measure of the maximum distance that water has to be transferred until it reaches the periphery of the specimen. f(X) is different for different specimen geometries. Some examples are:

* A water saturated slice with thickness D; Fig 7a.
  $f(X) = D^2/8$ (14)

* A water saturated sphere with diameter Φ; Fig 7b.
  $f(X) = \Phi^2/24$ (15)

* A water saturated shell with thickness L surrounding an air pore with the specific area α; Fig 7c. The outer periphery is impermeable. This is the model used by Powers /1949/ in his definition of the spacing factor.
  $f(X) = [L\cdot\alpha/9+1/2]\cdot L^2$ (16)

Thus, the hydraulic pressure will increase with increasing rate of ice formation, with increasing specimen size and with decreasing permeability. The concrete is damaged when the following condition is satisfied:

$$p_{max} = f_t \qquad (17)$$

Where f_t is the tensile strength of the concrete. Thus, there exist maximum material sizes or critical distances which must not be exceeded if the concrete shall be frost resistant. The following relations are valid for the three geometries in Fig 7:

* Water saturated slice:

$$D_{CR} = \{8 \cdot f_t \cdot K/(0{,}09 \cdot dW_f/dt)\}^{1/2} \qquad (18)$$

* Water saturated sphere:

$$\Phi_{CR} = \{24 \cdot f_t \cdot K/(0{,}09 \cdot dW_f/dt)\}^{1/2} \qquad (19)$$

* Water saturated shell or Powers´spacing factor:

$$L_{CR}^2\{L_{CR} \cdot \alpha/9+1/2\} = f_t \cdot K/(0{,}09 \cdot dW_f/dt) \qquad (20)$$

The value L_{CR} is also a function of the size of the air pore enclosed in the shell. Thus, L_{CR} is not the same true material property as D_{CR} and Φ_{CR}.

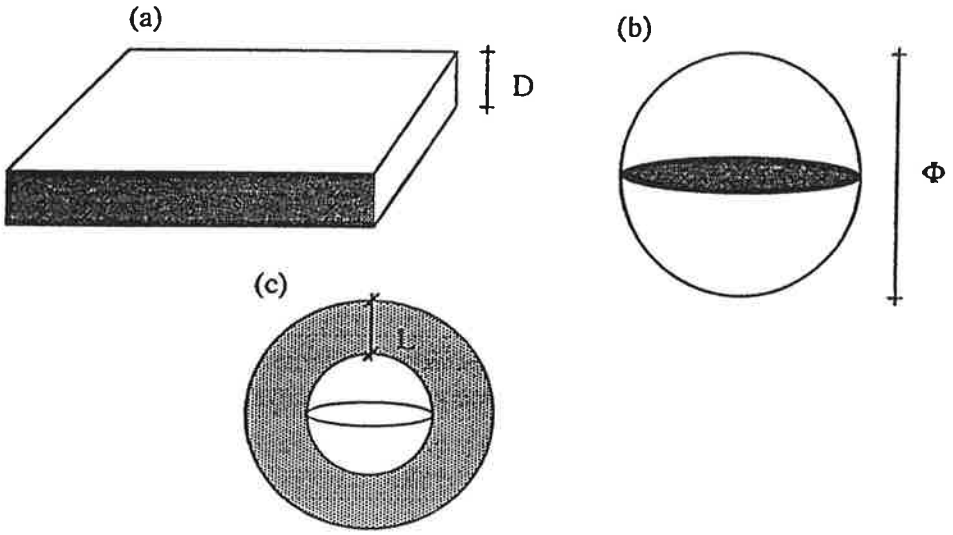

Fig 7: Different critical sizes.

Equations (18)-(20) show that geometrical relations between the different critical sizes exist. The relation between the critical thickness and the critical spacing factor is.

$$D_{CR} = 2 \cdot L_{CR}\{2 \cdot \alpha \cdot L_{CR}/9+1\}^{1/2} \qquad (21)$$

This relation is a function of the size of the spherical air pore inside the shell. A typical value of α for a concrete exposed to normal conditions is 15 mm^{-1}. Then, if the critical thickness is 1 mm the critical spacing factor is 0,35 mm. The critical spacing factor is therefore always smaller than the critical thickness.

The hydraulic pressure is only acting as long as new ice is formed. Therefore, it should vanish when the temperature is kept constant. The following relation is valid:

$$dW_f/dt = (dW_f/d\theta)\cdot(d\theta/dt) \qquad (22)$$

Where $dW_f/d\theta$ is a material function that is only dependent of the amount of ice formed at each temperature. Hence, $dW_f/d\theta$ is a function of the pore size distribution; c.f. eq (1). The function $d\theta/dt$ is the rate of temperature lowering of the specimen which is almost directly proportional to the rate of lowering of the outer temperature. Principally, one should therefore obtain a length-change/temperature curve of the type shown in Fig 8a when the temperature is kept constant during a certain time. Due to the lack of ice formation during this period the specimen should contract. In reality however one has obtained curves of the type seen in Fig 8b according to which the concrete length is almost constant when the temperature is constant. This does however not necessarily contradict the hydraulic pressure mechanism. There might be a certain ice formation despite the fact that the temperature is constant. The fact that the temperature is constant might depend on heat balance prevailing between latent heat developed during freezing and heat loss to the environment. Besides, one might imagine that ice that was formed at higher temperatures "lock" the material structure making it impossible for the specimen to contract. This is a special case of damage mechanism 1 which is described above. A further possibilty is that the material was permanently and irreversably damaged so that it cannot contract.

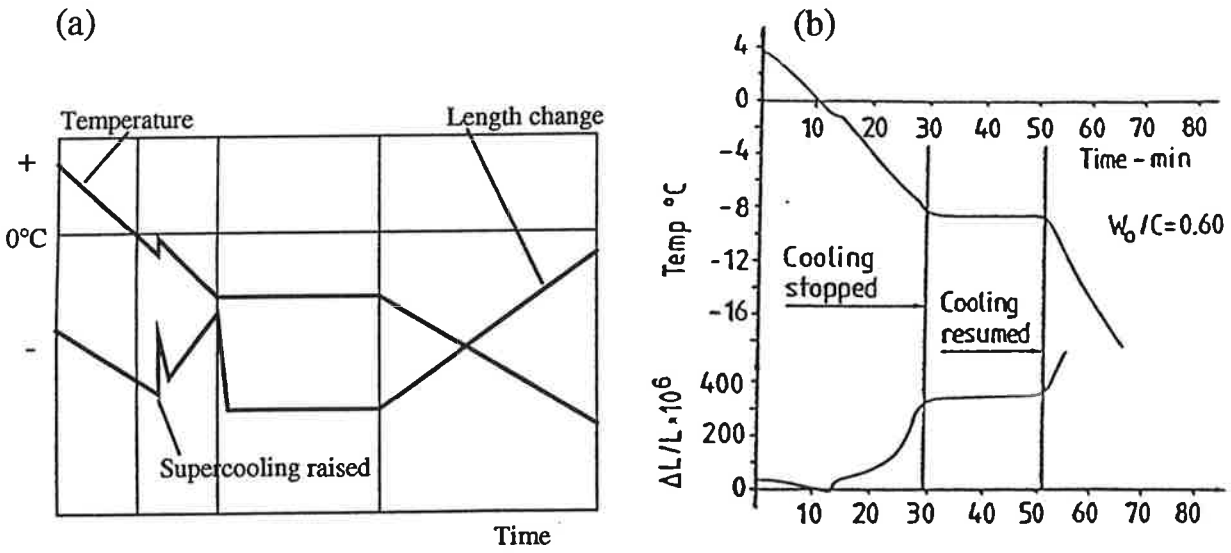

Fig 8: (a) Expected temperature-time and length-time curves at damage mechanism 2. (b) Measured temperature and length curves of a cement paste with the W/C-ratio 0,60. Powers & Helmuth /1953/.

According to the hydraulic pressure mechanism the pressure should be at its maximum when the rate of ice formation is at its maximum. This does normally occur in the beginning of the freezing process, at around 0°C. In the late stage the rate of ice formation is almost always much smaller. However, one must consider that the permeability is gradually decreased with decreased temperature due to the increased amount of ice formed inside the pore system. The reduced permeability might very well more than compensate for the reduced rate of ice formation. The fact that one often notices larger expansions of concrete at lower temperatures is therefore not necessarily a contradiction of the hydraulic pressure mechanism. This is visualized in Fig 9.

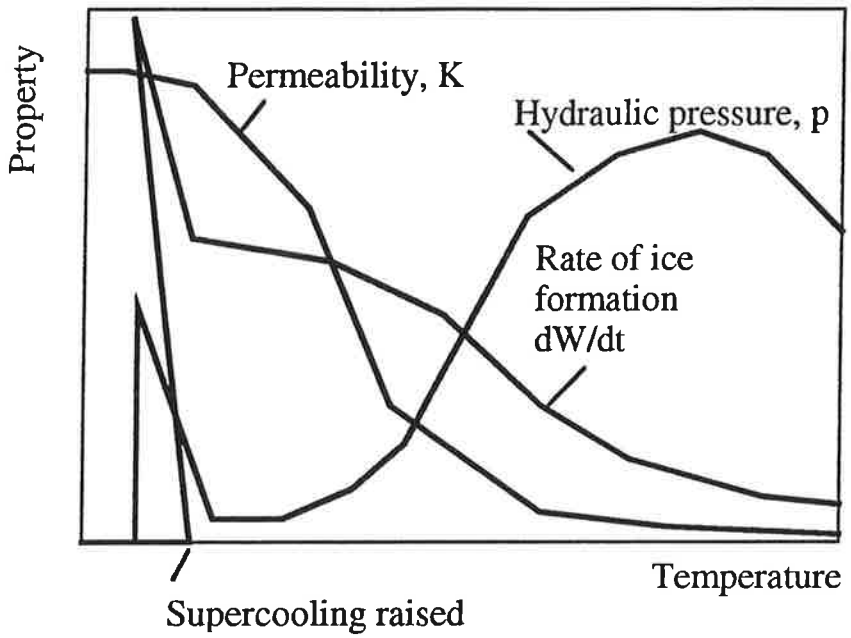

Fig 9: Hypothetical curves of the rate of ice formation, the permeability and the hydraulic pressure.

The critical size depends on the rate of ice formation which is almost directly proportional to the rate of temperature lowering of the surrounding air or water. Theoretically, according to eq(18) a doubling of the rate of temperature lowering gives a 30% reduction of the critical size. Damage mechanism 2 does therefore imply that the damage risk is increased with increasing rate of freezing.

The hydraulic pressure ought to decrease when the pore water is saline. The reason is that the amount of freezable water is decreased. Therefore, the critical size ought to increase somewhat.

The hydraulic pressure mechanism was initially elaborated by Powers /1949/.

Damage mechanism 2 is of special importance in two cases:

Case 1: The initial freezing. Due to supercooling, the pore water does not freeze until the concrete temperature is some degrees lower than the theoretical freezing point. This supercooling can be 5°C or more. When freezing suddenly

is initiated somewhere in the pore water it spreads rapidly over a large concrete volume containing supercooled water. Then, the concrete temperature rises momentarily to the real freezing temperature which is 0°C or a few degrees lower. A large amount of ice is formed during a few seconds and there is often a rapid expansion of the specimen. This expansion normally is reversible and is due to a "pumping effect" when a large amount of water is expelled to air-filled pores during a short time. In most cases, this expansion is not large enough to destroy the concrete. The largest expansion normally occurs at a later stage at lower temperatures; see Fig 9.

Case 2: Concrete with high W/C-ratio. In concrete with high W/C-ratio the freezable water content is higher than the non-freezable water content; see Table 2. Therefore, damage mechanism 3 described below cannot have the same significance as it might have in more fine-porous concretes. It is however not excluded that damage mechanism 2 is the dominant mechanism also for dense concretes with low W/C-ratio. The relative importance of damage mechanisms 2 and 3 has never been clarified.

2.4 Damage mechanism 3; Microscopic ice lens growth

Every concrete will, due to its fine pore structure, at the same time contain ice bodies in the coarser capillaries and in certain air pores and unfrozen water in the finest capillaries and in the gel pores. The lower the W/C-ratio the larger the fraction of unfrozen water. This co-existence of water and ice makes a damage mechanism possible that is similar to the mechanism that causes frost heave in the ground. At any temperature below 0°C unfrozen water has a higher free energy content than ice. The ice bodies will therefore attract water and one obtains a water transfer towards the freezing site. The microscopic ice bodies in the capillaries will grow and thereby expose the pore walls to pressure. This means that the ice will also be exposed to pressure. The free energy of the ice body will therefore increase at the same time as the free energy of the unfrozen water will decrease due to the drying effect caused by the water transfer. The growth of the ice body or "ice lens" will not cease until the the free energy of the ice is high enough to balance the free energy of the remaining unfrozen water. Before this occurs, pressures high enough to seriously damage the concrete can probably be built up. This is shown by the calculations below. The damage mechanism is visualized in Fig 10.

It is difficult to quantify the pressure. It depends on the type of meniscus systems that appear inside the concrete. It also depends on how big the drying effect will be. The more unfrozen water in relatively coarse pores the larger water transfer is possible and the larger pressures can be built up. For the idealized case in Fig 11a in which an isolated ice lens surrounded by unfrozen water has access to unlimited amount of water the following expression is valid.

$$p = (\Delta H/T)\cdot[\Delta\theta/(v_i - v_w)] \qquad (23)$$

Where

p	the pressure between the ice body and the pore wall (Pa)
ΔH	the molar latent heat of fusion ($6 \cdot 10^6$ J/kmole)
T	the actual temperature (T=273,15-$\Delta\theta$ °K)
$\Delta\theta$	the actual freezing point depression of unfrozen water (°K)
v_i	the molar volume of ice ($19{,}8 \cdot 10^{-3}$ m^3/kmole)
v_w	the molar volume of liquid water ($18 \cdot 10^{-3}$ m^3/kmole)

Thus, the pressure will increase with decreasing temperature. At -20°C the pressure is 260 MPa.

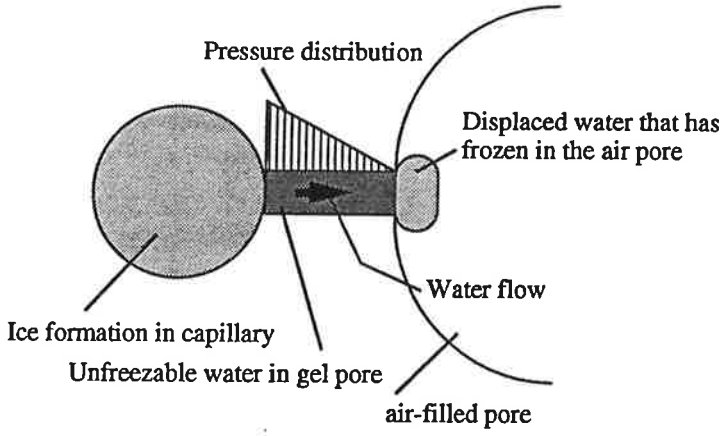

Fig 10: Illustration of damage mechanism 3.

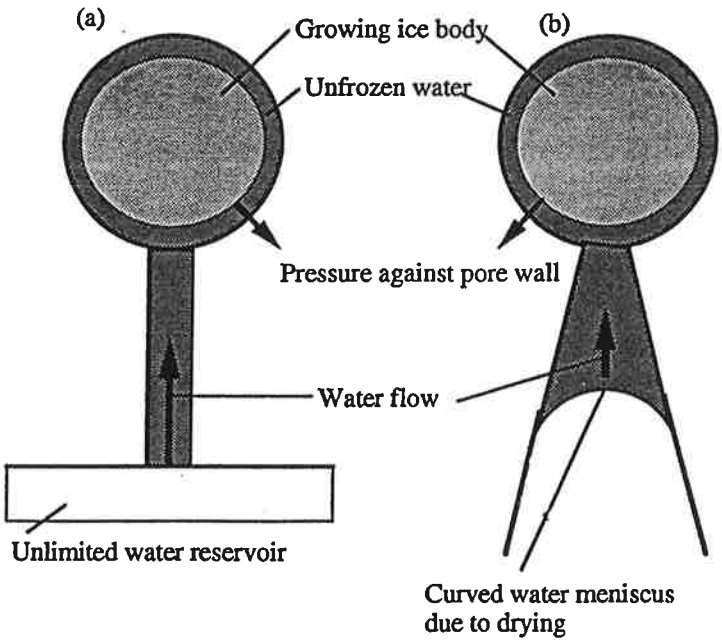

Fig 11: Model for calculating the pressure caused by microscopic ice lens growth. (A) Unlimited supply of unfrozen water. (b) Limited amount of unfrozen water; the drying effect.

Powers /1956/ treats the case where the pressure from the ice body acts directly against the pore wall. This leads to considerably lower pressures which can however still be big enough to cause damage.

Drying due to transfer of non-freezable water reduces the pressure. The following expression can be used for the model in Fig 10b.

$$p = (\Delta H/T)\cdot[\Delta\theta/(v_i - v_w)] - [v_w/(v_i - v_w)]\cdot p_d \qquad (24)$$

Where the second term on the right hand side is the reduction due to desiccation. p_d is the under-pressure in the water phase caused by drying. It depends on the curvature of the meniscus between water and air and can be described by the Laplace law:

$$p_d = 2\cdot\sigma/r_d \qquad (25)$$

Where

σ	the surface tension between air and water ($75\cdot10^{-3}$ N/m)
r_d	the radius of the meniscus between air and water (m)

Let us assume that the temperature is -20°C as in the example above and that the drying has created an under-pressure which can be described by the meniscus radius 70Å corresponding to 85% RH according to the Kelvin equation. The pressure excerted by the ice body is now reduced from 260 MPa to about 45 MPa.

Pressure due to this mechanism appears as long as water transport to the ice lens is possible; i.e. as long as there is no energy balance between ice and water. Therefore pressure can appear even when there is no lowering of the temperature. One practical example of this feature is seen in Fig 12.

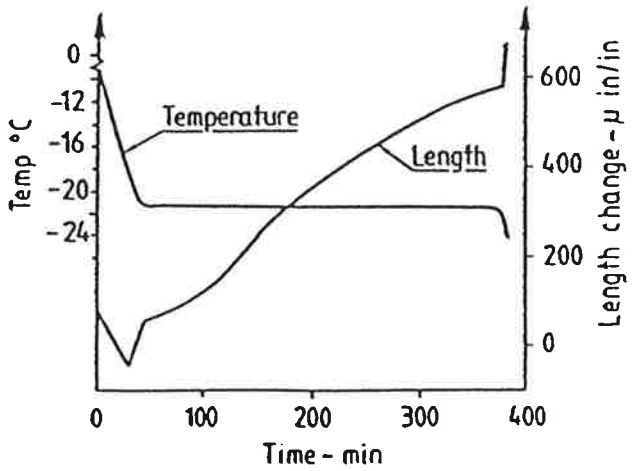

Fig 12: Measured temperature-time and length-time curves at freezing of a cement paste with the W/C-ratio 0,45. Powers & Helmuth /1953/.

During the very first freezing taking place around 0°C some water is transferred by hydraulic action to the air pores where it will freeze momentarily. Growth of these ice bodies will occur without pressure being excerted. Water transfer therefore primarily takes place towards these ice bodies. After a certain time other ice bodies being under pressure will melt and the melted water will be transferred towards the stress-free ice in air pores. Therefore, the maximum pressure appearing in the cement paste depends on the possibility of water transfer towards air pores. The pressure will diminish when the distance between air pores is decreased. Damage mechanism 3 therefore also predicts the existence of critical distances, e.g critical thicknesses or critical spacing factors. This statement is supported by measurements; see Fig 13b showing length measurements of cement paste with different spacing factors. The larger the spacing factor the more the cement paste during the freezing phase expands . At very low spacing factors a considerable contraction takes place. This is probably due to the fact that the contraction caused by water transfer dominates over the the pressure from the growing ice lenses; the second term on the right hand side of eq (24) dominates over the first term.

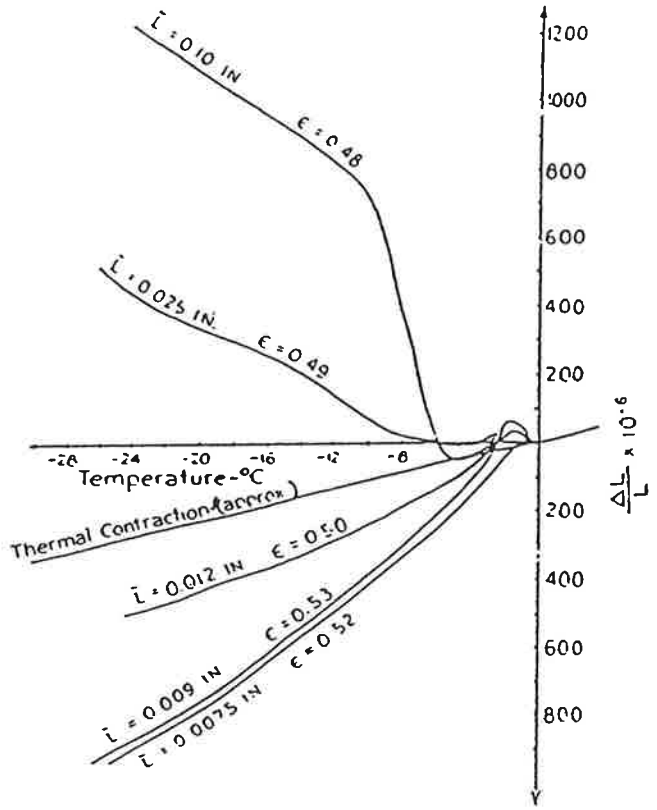

Fig 13: Effect of the Powers´spacing factor on the length change at freezing of a cement pastes with the W/C-ratio 0,60. Powers & Helmuth /1953/. (The spacing factor is given in inches. ε= the amount of evaporable water (m^3/m^3). The cooling rate is 0,25 °C per hour.)

Theoretically, damage mechanism 3 ought to be more pronounced the lower the freezing rate and the longer the freezing period. Then, the pressure has more time to develop. This is a great difference between damage mechanisms 3 and 2. The latter is favoured by a rapid freezing.

The pressure ought to increase when the pore water is saline. When some of the water in a coarse pore freeezes the salt concentration of the unfrozen part of the solution in the same pore increases. Diffusion of salt water in cement paste is slower than diffusion of pure water. Therefore, a concentration gradient appears in a pore containing an ice body and finer pores containing only the initial solution. The cement paste acts as a semi-permeable membrane and an osmotic pressure is built up and is added to the normal pressure in a salt-free system. At high salt concentrations the total amount of freezable water is, however, reduced which is a positive factor. One can therefore assume that the highest pressures occur at a certain pessimum inner salt concentration. This is visualized in Fig 14 in which hypothetical relations between the inner salt concentration and the internal pressure are indicated.

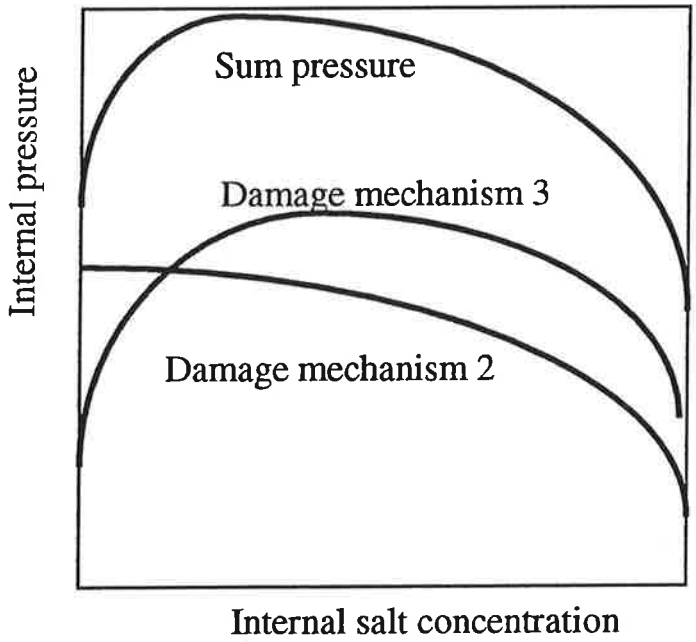

Fig 14: Hypothetical effect of the inner salt concentration on the pressures due to damage mechanisms 2 and 3 ,together with the sum effect.

An experimental determination of the expansion of cement mortar prisms containing pore water with 4 different NaCl-concentrations is shown in Fig 15. The degree of saturation is almost the same in all prisms. In the experiment shown in Fig 15 as in all the other experiments performed the salt concentration 2,5% gave the largest expansions while the concentration 10% gave about the same expansion as pure water or even less expansion. The damage mechanism has been treated by many authors. The first application to concrete was made by Powers & Helmuth /1953/.

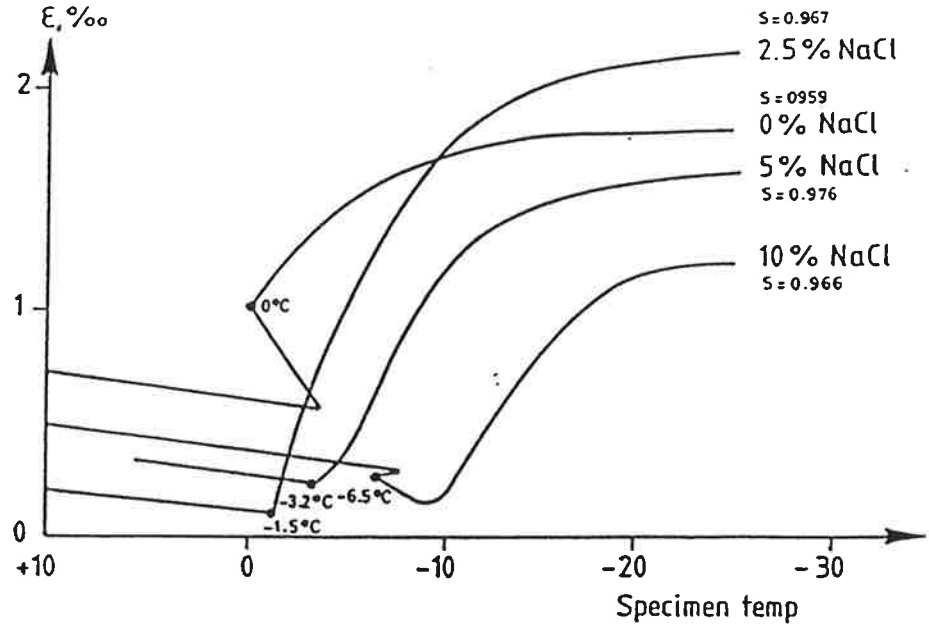

Fig 15: Measured length changes of cement mortars containing pore solutions of different strengths expressed as % NaCl. The degree of saturation is almost the same in all concretes. Fagerlund /1992/.

Damage mechanism 3 is of importance in at least two cases:

Case 1: Concrete with low W/C-ratio. Such concretes have large amounts of non-freezable water; see Table 2. This means that large pressures can be built up before the drying effect limits the pressure.

Case 2: Freezing with saline pore water. This is treated above.

2.5 Damage mechanism 4; Macroscopic ice lens growth

This mechanism is exactly the same as that causing frost heave in the ground. The mechanism requires that a stable (immobile) ice formation front arise in the concrete for example at its surface part and that this front is continuously supplied by water from a "reservoir" located to the unfrozen part of the concrete or outside of this. The mechanism is illustrated by Fig 16a.

The ice front or the zero-degree front lies still when energy balance prevails; heat that is transferred to the front as a sum of the capacitive heat and the heat of ice formation of water migrating to the front must be exactly as high as the heat loss from the front to the surroundings. Therefore, the first condition for macroscopic ice lens growth can be formulated:

$$dQ/dt = \{dQ/dt\}_f + \{dQ/dt\}_c \quad (26)$$

Where

dQ/dt	the heat flow from the ice front (J/s)
$\{dQdt\}_f$	the latent heat at freezing of water transferred to the ice front (J/s)
$\{dQ/dt\}_c$	the heat capacity of water transferred to the ice front (J/s)

The two fluxes on the right hand side are determined by the permeability of the concrete and by the driving force. This is of exactly the same typ as for destruction mechanism 3; i.e. energy differences between ice and unfrozen water. In mechanism 4 the driving force is strengthened since the water is always warmer than the ice.

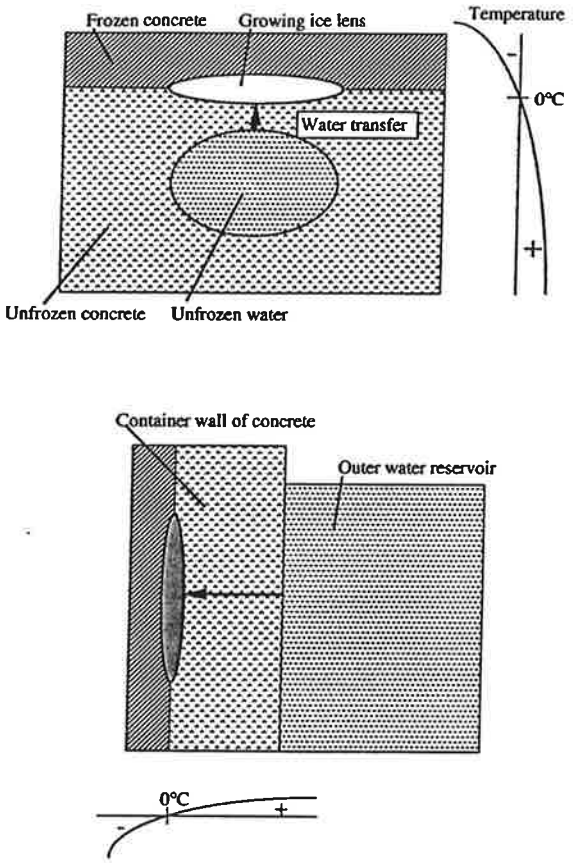

Fig 16: Illustration of damage mechanism 4.

When the permeability is too low the ice front can no longer be supplied with water and the ice front will advance and the ice lens segregation accordingly will cease. Powers /1956/ postulates that the ice lens segregation should cease when the permeability of the concrete defined by eq (27) is smaller than $50 \cdot 10^{-12}$ s. Values similar to this have been calculated by Fagerlund /1980/ for the case macroscopic ice lens growth in green concrete. The exact value of the critical permeability depends on the outer temperature conditions. When it is very cold outside the structure the heat loss to the environment is high and consequently the permeability must be high if the ice lens segregation shall be possible.

$$dq/dt = B \cdot dp/dx \qquad (27)$$

Where

dq/dt	the water flux [kg/(m^2·s)]
dp/dx	the pressure gradient [N/(m^2·m)]
B	the coefficient of permeability (s)

The permeability levels just discussed are valid when water is only transported by energy differentials. Ice lens growth can occur at much lower permeabilities if water is also transported by outer water pressure; Fig 16b. A normal well-cured out-door concrete is however dense enough to make ice lens growth impossible even during such conditions.

The driving force diminishes if the concrete is drying. The mechanism is exactly the same as that described under damage mechanism 3 above; eq (24)

A second condition for macroscopic ice lens growth is that the pressure in the ice lens is not so high that the lens penetrates an adjacent entrance pore instead of growing in situ. This condition is given by the following relation which was derived by Penner /1958/

$$p_{max} = 3{,}75 \cdot 10^9 \{1-\exp(-4{,}54 \cdot 10^{-10}/r)\} \qquad (28)$$

Where r (m) is the fictitious radius of an equivalent cylindrical entrance pore.

Damage can therefore be hindered if the concrete strength exceeds a certain value given indirectly by eq (28). Similarly, frost heave in roads can be stopped by exposing the ground to a pressure which is high enough.

Already before the pressure given by eq (28) is reached a stress relief can be obtained if the growing ice body can force the previously formed ice out of the material towards its warm face. For some coarse-porous materials such as clay brick one has observed long "ice worms" coming out from the pores at the warm face. In such cases the material has had access to large amounts of unfrozen water during a long period.

The diameter of the coarsest pore in a concrete will probably always be smaller than 1 µm. Therefore, according to eq (28), a pressure of 3,4 MPa or more can arise before ice lens growth is stopped. Even before that happens the permeability criterion is normally "activated". A concrete with very low tensile strength and high permeability can however become damaged by macroscopic ice lens growth especially if the concrete is exposed to outer water pressure like in Fig 16b. This has been observed by Collins /1944/.

The mechanism was for the first time explained theoretically by Beskow /1935/. The first application of the theory to concrete was made by Powers /1956/.

The damage mechanism 4 is of special importance in two cases:

Case 1: Green concrete. Normally, all criterions for macroscopic ice lens growth are fulfilled in a concrete that freezes a short time after casting. The ice formation occurs immediately below the surface that is cold while the interior of the concrete, which is warmer, supplies the water so that the ice lens can grow almost without restraint. The growth does not cease until the permeability is reduced below the critical value due to hydration or until the interior of the concrete is dried so much that heat balance according to eq (26) can no longer be maintained. The ice lenses are often formed at the interfaces between coarse aggregate grains and the cement paste. Delaminations have also been observed; Johansson /1976/.

Case 2: Concrete of low quality in hydraulic structures such as dams. In this case the water reservoir on the warmer side provides the water required for the ice lens growth. In the worst case the concrete can be totally delaminated.

3 The critical fictitious spacing factor

3.1 Definition

The two major destruction mechanisms 2 and 3 described above predict the existence of critical sizes such as a critical thickness D_{CR} of a saturated slice of the cement paste or a critical thickness L_{CR} of a saturated cement paste shell surrounding an air pore . The latter is normally expressed in terms of the so called Powers´spacing factor which is based on the model shown in Fig 17. All air pores are supposed to have the same size and to be arranged in a cubic array consisting of cement paste and air pores. The spacing factor is the distance between the corner of the cube and the periphery of the air pore. It therefore corresponds to the longest distance that water expelled from the freezing site has to be transferred. It is easy to derive the following geometrical relation between the spacing factor and the air pore parameters:

$$L_f = \{1{,}4[V_p/a+1]^{1/3} - 1\}3/\alpha \qquad (29)$$

Where

L_f	the fictitious Powers´spacing factor (mm)
V_p	the cement paste volume except air pores (m^3/m^3 or %)
a	the total air content (m^3/m^3 or %)
α	the specific area of the total air pore system (mm^{-1})

By the wordings "fictitious spacing factor " and "total air pore system" is meant that all air pores are included. Even such pores that become water-filled during a practical freeze/thaw test or in the practical situation in the field. In V_p could

also be included sand grains that are small enough to interfere with the air pores, i.e grains smaller than about 0,5 mm.

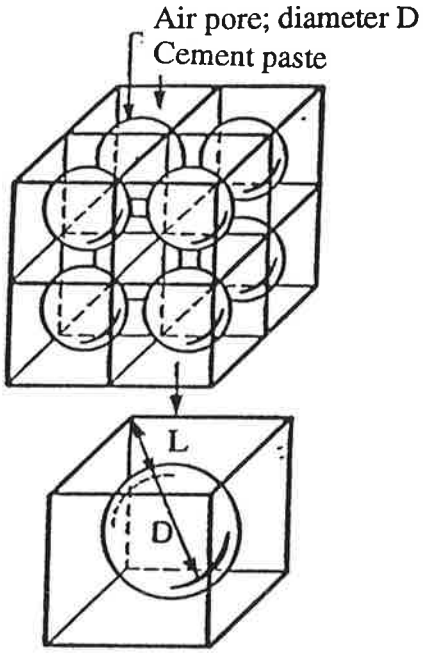

Fig 17: Model defining the Powers´spacing factor. Powers /1949/.

Note: The geometrical model behind the Powers´spacing factor is unrealistic. In reality the air pores are of different size and are arbitrarily distributed over the cement paste volume. A much better spacing factor concept is the Philleo spacing factor which expresses a distance which is within a certain probability equal to or bigger than the distance from any arbitrary point in the cement paste to the nearest air pore; Philleo /1955/. A spacing factor of the similar type bur derived according to another theoretical model in which consideration can also be taken to the actual air pore size distribution was derived by Fagerlund /1977/. The following relation is valid for the case that there is 63% probability that any given point in the cement paste shall be within the distance d from the periphery of an air pore:

$$a\{1+0,5\cdot d\cdot\alpha+0,5\cdot d^2\cdot\alpha\cdot[u]_1/[u]_2+0,17\cdot d^3\cdot\alpha\cdot[u]_0/[u]_2\}=1 \qquad (30)$$

Where

a	the air content (m^3/m^3)
α	the specific area of the entire air pore system (mm^{-1})
d	the distance between any point and the nearest air pore (mm)
$[u]_i$	the i:th statistical moment of the air pore distribution

One can also select a higher probability than 63%. Then the spacing factor d is reduced.

3.2 Experimental technique

The critical fictitious spacing factor is determined by comparing the results of freeze-thaw tests with spacing factors determined by analyses of the pore structure of companion specimens. By plotting the damage versus the fictitious spa-

cing factor a critical value can sometimes be found below which little damage occur and above which damage is normally substantial. Results of such plots are shown below.

The freeze-thaw experiment can be designed in many different ways; e.g.:

* Freezing in air, thawing in water
* Freezing and thawing in water
* Freezing and thawing in salt solution
* Freezing in water, thawing in salt solution
* Slow freezing
* Rapid freezing
* Slow thawing
* Rapid thawing
* etc

The result will to a large extent depend on the manner by which the test is performed; (i) if the freezing rate is changed the internal stresses are changed which must have a certain influence on the results of the test; (ii) if the test is made more "wet", meaning that the specimen has better possibilities to absorb water during the test, a larger amount of air pores become water-filled; (iii) if the specimen is exposed to salt at its surface during the test the internal stresses are very much augmented due to increased water ingress; etc.

The fictitious spacing factor is determined by a microscopic analysis af a cross section of the concrete. This can be done by the manual so called linear traverse technique (ASTM C457) or by automatic image analysis. Only pores with diameter larger than 5 to 10 μm are registered and used in the calculations. Smaller pores are very rapidly inactivated by water absorption. There is a certain effect on the calculated spacing factor if the size distribution is cut at 5 μm or at 10 μm or perhaps even at 20 μm. In many pore systems there is a large number of very small pores. Therefore, the contribution to the specific area of the smallest pores can be significant although the effect on the total air content is negligible. According to eq (29) the specific area is inversely proportional to the fictitious spacing factor.

Due to all the possible variations in test procedures one cannot expect to get a very well-defined value of the critical fictitious spacing factor.

It must also be noticed that the spacing factor is not a true material property since it depnds on the size of the air pore enclosed by the cement paste shell; cf eq (20). The critical thickness is more of a true material property.

3.3 The critical fictitious spacing factor at salt scaling

3.3.1 Main study; many variables in mix design and compaction

In a test series performed by Lindmark /1993/ a certain concrete with "average" salt scaling resistance was tested in a number of ways in order to find out the effect of different test parameters on the frost damage. The following variables were investigated; (i) the inner salt concentration; (ii) the outer salt concentration ; (iii) the lowest freezing temperature; (iv) the freezing rate. 5 cm thick slices of the concrete were pre-stored for 9 months in either pure water or in 3% or 6% NaCl-solution. Then, they were freeze-thaw tested with either pure water or 3% or 6% NaCl-solution poured in a "basin" on the top surface of the specimen. Thus, 9 combinations of outer and inner salt concentration were investigated. The specimens were exposed to 56 cycles of freeze-thaw. Each cycle was composed of 16 hours of freezing to the minimum temperature and 8 hours of thawing to room temperature. Three minimum temperatures were used; -7°C, -14°C and -22°C. Two freezing rates were used; "rapid" and "slow". The results showed that two parameters were dominant; see Fig 18.

1: The minimum freezing temperature: Only -22°C gave severe damage while -7°C almost gave no damage irrespectively of the other variables.

2: The outer salt concentration: 3% salt concentration outside the concrete always gave more damage than any other outer and inner concentration. The inner concentration had a marginal effect.

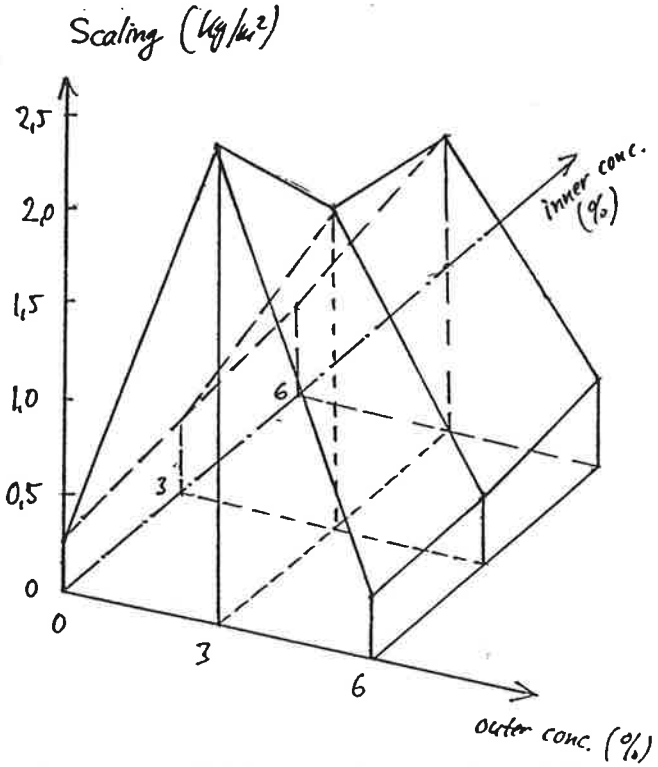

Fig 18: The salt scaling after 56 freeze-thaw cycles of the same concrete but with different outer and inner salt concentrations. Minimum temperature -22 °C. "Rapid" freezing. Lindmark /1993/.

It therefore seems reasonable to assume that a lowest value of the critical fictitiuos spacing factor is obtained when it is based on a freezing experiment with about 3% outer NaCl-concentration and a minimum temperature below -20°C. The freezing rate has a certain influence and should correspond to the maximum rate in practice.

A large number of concretes (about 600 specimens) have been freeze-tested according to these principles. The W/C-ratio was 0,45 in all concretes. The air content varied over a large span; from no air-entrainment to more than 8% air content. Many different air entraining agents and many different water reducing agents or superplasticizers were used. The slump value varied from stiff to very fluid. The concretes from which the freeze test specimens were taken were compacted in four different ways; no vibration, fall table compaction, table vibration, poker vibration. Therefore, different air losses were obtained for the same concrete. Only one type of cement was used. It was an OPC with 5% limestone filler, C_3A-content 8% and water soluble alkali content 0,6%.

Most concretes were water-cured for 3 months from the day after casting. During this period the specimens were prepared by cutting 25 mm slices from cast cylinders with diameter 10 cm. During the last three weeks before freeze-thaw testing the slices were dried in laboratory air during two weeks followed by water storage during one week. This means that the concretes had went through a drying-wetting cycle but that they were wet when the test started. During the drying period the edge of the slice was sealed by silicone rubber. The sawn surface was used as test surface.

The storage during the freeze-test is shown in Fig 19. The slice was placed on the edge of a plastic petri cup which was in turn placed in a bigger petri cup. 3% NaCl-solution was poured in the cups so that about 2 mm of the specimen was immersed. The lid of the outer petri cup was provided with a hole suiting the specimen and was then put in place. The lid is necessary in order to protect the solution from evaporation .

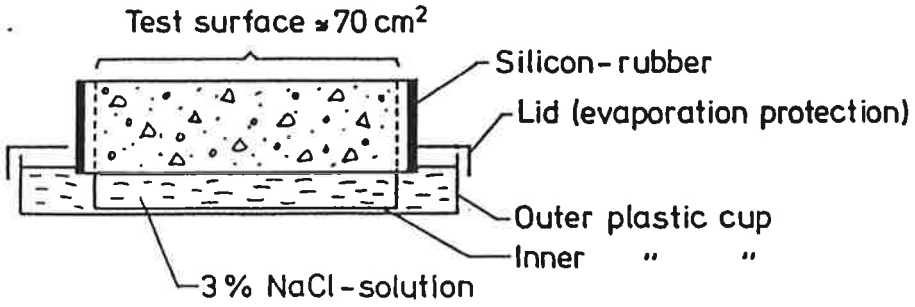

Fig 19: The salt scaling test.

All specimens were placed in an automatic test cabinet in which they were exposed to freeze-thaw cycles.The freeze-thaw cycle consisted of 16 hours freezing to about -18 to -20°C and 8 hours heating to room temperature. The free-

ze-thaw cycling caused scaling of the bottom face of the specimen. The scaled particles were collected in the inner petri cup. With about 7 cycles interval the specimens were taken out and the scaling was collected, dried at +105°C and weighed. The salt solution was renewed and a new series of 7 freeze-thaw cycles started. The total number of cycles varied. Some concretes were converted to "gravel" after a few cycles. other were more or less unharmed after 56 cycles. Normally 28 to 35 cycles were used.

The scaling is expressed in kg/m^2 based on the exposed surface (the area of the inner cup) and plotted versus the number of cycles. Some results are shown in Fig 20. A concrete with fair salt scaling resistance shall have a linear or retarded scaling; i.e. the scaling during the last 14 cycles shall be smaller than the scaling during the first 14 cycles. It is difficult to give a distinct criterion for what is an acceptable level of scaling. It was found however that the scaling was retarded in almost all cases when the total scaling after 28 cycles was less than 0,6 kg/m^2. This is therefore used as criterion. It can be mentioned that the Swedish standard test method for salt scaling -"the Borås method"- uses the limit 1 kg/m^2 after 56 cycles and 0,5 kg/m^2 after 28 cycles for the damage degree "acceptable scaling".

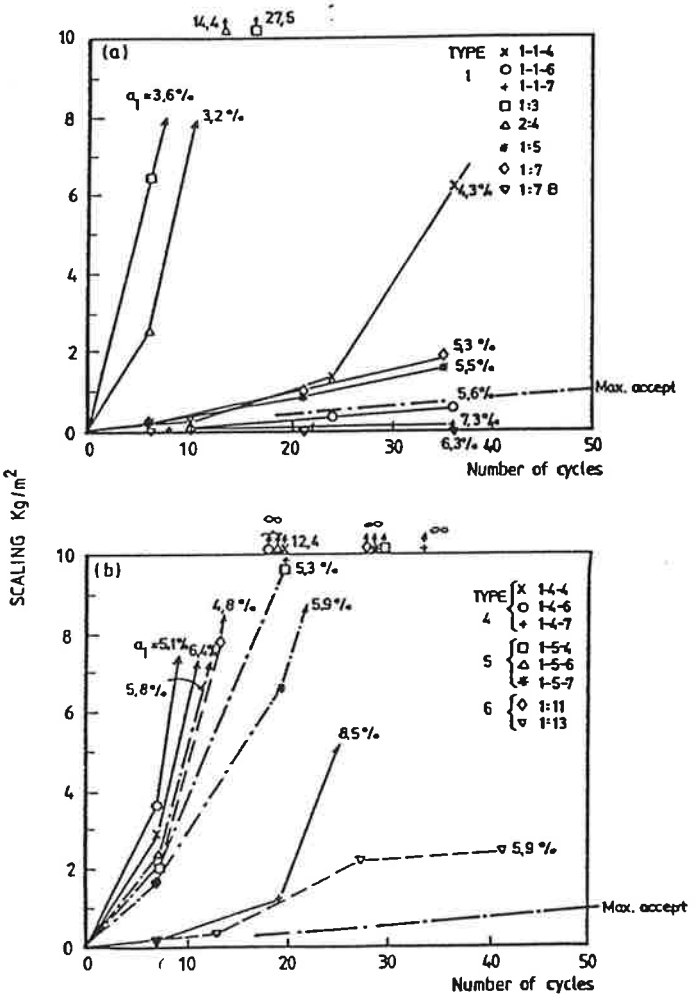

Fig 20: Examples of the result of the salt scaling test. Different concretes made with different air entraining admixtures. The air content of the fresh concrete is marked on the curves. (a) Neutralized Vinsol Resin. (b) Combined air entraining and water reducing agents.

Companion specimens of a number of different concretes were sent to the Technological Institute in Denmark where they were studied by automatic image analysis. The analysis was made on polished saw cuts which were painted black by stamp ink. The small air pore callottes in the surface were made visible by scraping a zinc-white paste over the surface. Thus, all the air pores appear as white circular spots on a black background. The prepared specimen was placed in the image analysing equipment where the size distribution, the air content, the specific area and the spacing fator of the air pore system is obtained automatically. In calculating the spacing factor it is assumed that the cement paste fraction in the section studied is the same as in the concrete in bulk. The real paste content in the section could not be quantified be the technique used. The mathematical treatment is the same as in the manual ASTM method; ASTM C457. The results could therefore be compared with results found in earler tests by other authors. It must be noticed that the resolution in the microscopic technique used is very high.

A plot of the total scaling after 28 freeze-thaw cycles and the measured fictitious spacing factor is seen in Fig 21. Every point in the diagram is the mean value of the scaling of 3 specimens. Most concretes suffered severe scaling. Many were completely destroyed. Some specimens were severely damaged despite a spacing factor as low as 0,16 to 0,18 mm. On the other hand there are specimens with the rather big spacing factor 0,22 mm but with very low scaling. Therefore, it is a bit difficult to identify a general value of a critical fictitious spacing factor. It is quite evident that other factors than the spacing factor are also important for the scaling resistance. One such factor is the ability of the airpore system to absorb water. One can imagine that some air pore systems are fine-porous with low spacing factors but with a high ability to absorb water. Other pore-systems are more coarse having a higher value of the spacing factor but they stay air-filled.

The critical fictitious spacing factor lies wihtin a certain interval:

$L_{f,CR}$ = 0,16 to 0,22 mm

For safety reasons the smallest value ought to be used. It must be noticed that the values might be a bit smaller than what had been the case if a normal resolution had been used in the microscopic technique. It might be that 0,16 mm corresponds to about 0,18 mm with a resloution which is used in the traditional linear traverse technique.

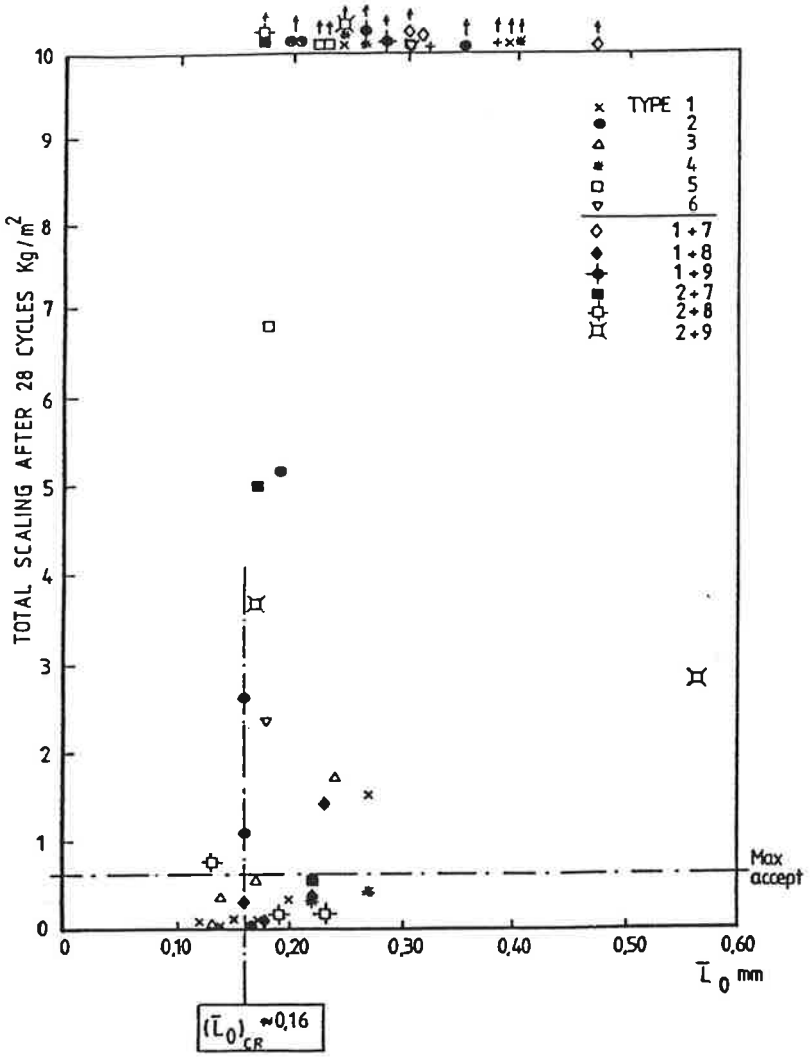

Fig 21: Main study: Relation between the fictitious spacing factor and the salt scaling after 28 freeze-thaw cycles.

3.3.2 Special study 1; effect of the air content

In a limited study only the effect of the air content on the salt scaling was investigated. The cement type (the same OPC as in the main study), the air entraining agent (Neutralized Vinsol Resin), the curing and all other parameters except the air content were kept constant. No water reducing agent was used which certainly contributed to the small spread in the results. The specimens were water cured for 3 months before the test procedures involving pre-drying, rewetting etc, started. The freeze-test procedure was exactly the same as that described above in 3.3.1. The specimens were sawn from the top of cast cylinders. The sawn surface was used as test surface.

The air pore analysis was made by the manual linear traverse method desribed in ASTM C457. The specimens were polished in kerosene until a fineness was reached that corresponds to the quality criterion in the standard The linear traverse equipment and its precision is described in Warris /1963/. The smallest air void registered was about 5 μm.

A plot of the spacing factor versus the scaling after 28 freeze-thaw cycles is shown in Fig 22. Every point in the diagram is the mean value of the scaling of three specimens. The relation is rather linear; the larger the spacing factor the larger the scaling. The well-defined relation is probably a consequence of the fact that only one parameter -the air content- was varied in the test.

The critical fictitious spacing factor corresponding to a scaling of 0,6 kg/m^2 after 28 cycles of freezing and thawing is:

$L_{f,CR}$ = 0,18 mm

Thus the value is a bit larger than the smallest value found in the main study.

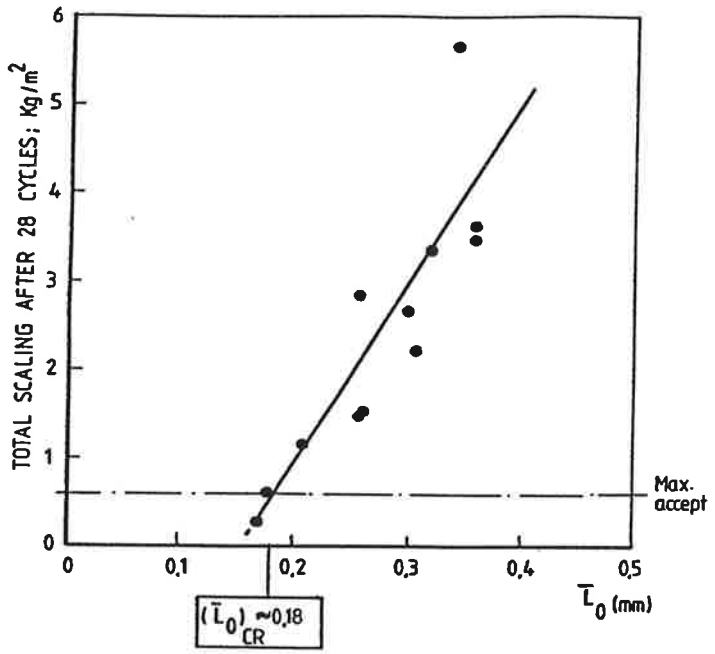

Fig 22: Special study 1: Relation between the fictitious spacing factor and the total salt scaling after 28 freeze-thaw cycles.

3.3.3 Special study 2; effect of the cement type

In a special study the effect of the type of binder was analysed. The cement was of four types with varying amount of ground garanulated blast furnace slag (GBFS).

* Type A: 100% OPC
* Type B: 85% OPC+15% GBFS
* Type C: 60% OPC+40%GBFS
* Type D: 35% OPC+65% GBFS

The OPC characteristics are: limestone filler 5%, C_3A content 8%, water soluble alkali content 1,1%.

The air-entraining agent was of type Neutralized Vinsol Resin. No water reducing agent was used. Three different nominal air contents were used for every cement type; the real air content differed a bit from the nominal:

* no air entrainment (1-2%)
* 4,5 %
* 6%

All concretes had the W/C-ratio 0,45. They were water cured during 3 months and were then exposed to the same test procedure as in the main study and in the special study 1. The specimens were sawn from the top of cast cylinders. The sawn surface was used as test surface. The air pore analysis was performed by the same automatic technique as that used in the main study.

Results of the scaling test as function of the air content are shown in Fig 23. The scaling is always reduced when the air content is increased. With high slag content the scaling resistance is fairly good even at rather low air contents.

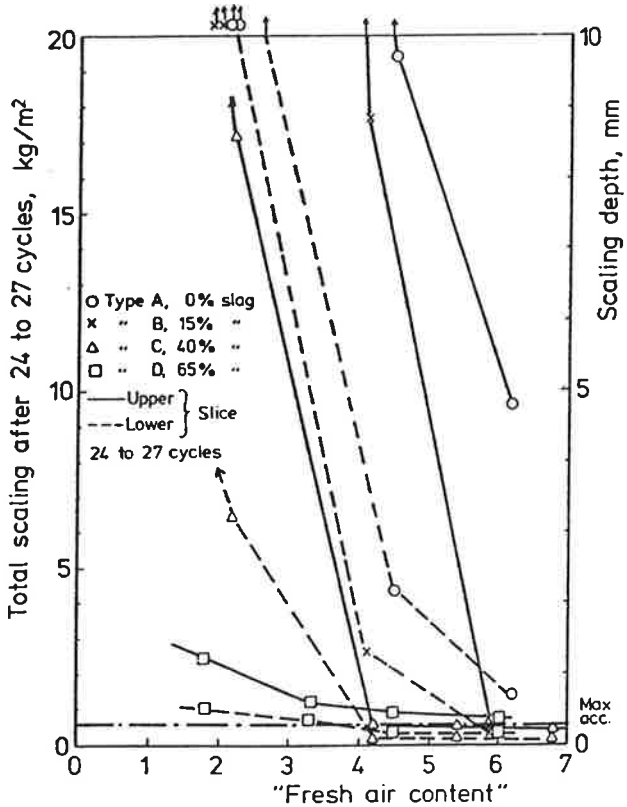

Fig 23: Special study 2: The salt scaling after 27 freeze-thaw cycles versus the air content of the fresh concrete.

In Fig 24 a plot of the scaling after 27 freeze-thaw cycles versus the spacing factor is shown. The results are difficult to interprete. It is quite clear that a reduction in the spacing factor gives a reduction in the scaling. However the spacing factors required are very low and seem to be depending on the type of ce-

ment. The critical fictitious spacing factor lies within a certain interval:

$L_{f,CR}$ = 0,10 to 0,13 mm

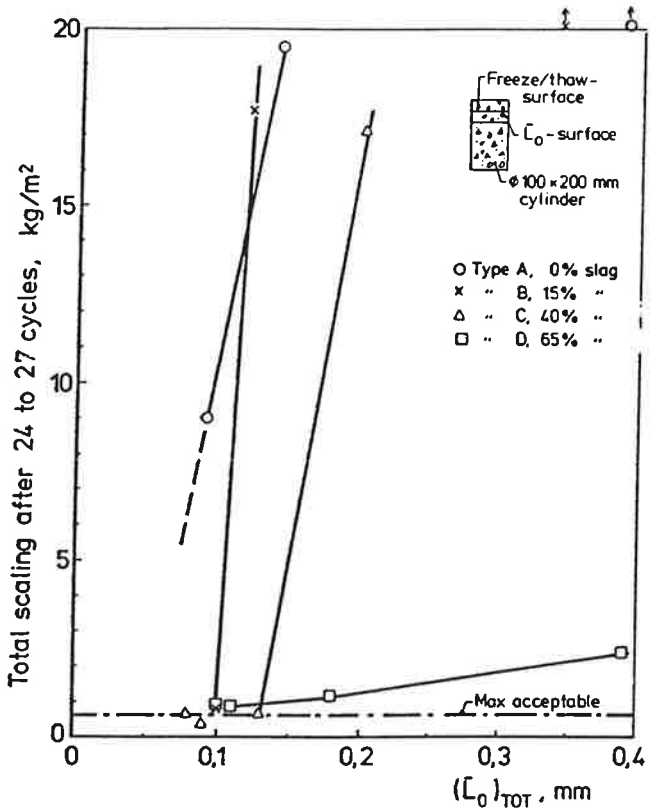

Fig 24: Special study 2: Relation between the fictitious spacing factor and the salt scaling after 27 freeze-thaw cycles.

The values are very low. One possible explanation is that the air pore structure was unstable due to the chemical characteristics of the OPC part of the cement. Unusually large air-losses were observed when the concretes were exposed to prolonged poker vibration; see Fig 25. It has been observed in other studies that this OPC gives very variable scaling resistance even at high air contents; Fagerlund /1983/, Malmström /1990/. One reason could be the combination of high alkalinity and Neutralized Vinsol Resin. It was found already by Mielentz et al /1958/ that a high alkalinity of the cement might give inferior air pore systems when Vinsol Resin is used. This has also been confirmed by air pore analyses and freezing experiments performed by Pistilli /1983/. Therefore, one cannot exclude that the air pores in the tested specimens were not isolated but more or less continuous making it possible for water to enter during the test. This shows the risk of utilizing the fictitious spacing factor instead of the real spacing factor. In the latter, only pores that stay air-filled are included.

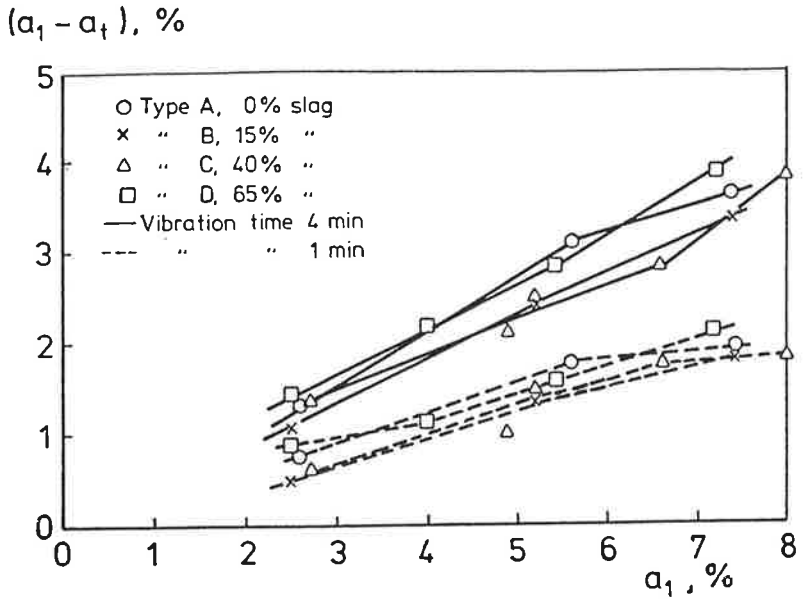

Fig 25: Special study 2: The air-loss after 1 and 4 minutes poker vibration versus the air content determined after standardized table vibration.

3.3.4 Special study 3; effect of the type of air-entraining agent

In a special study the effect of two types of air-entraining agents on the salt scaling resistance was tested:

* Type A: a pure air-entraining agent of type Neutralized Vinsol Resin
* Type AW: a combined air-entraining and water reducing agent based on a mix of lignosulfonate and Neutralized Vinsol Resin

The cement was the same OPC as in Special study 2. 4 different nominal air contents of the fresh concrete were aimed at; the real air content is a bit different:

* no air-entrainment
* 3,5%
* 4,5%
* 6%

The cylinder specimens were cast from concrete that had been pre-compacted by poker vibration in a full-scale wall-form. The test slices were cut from the top part of the cylinders. The sawn surface was used as test surface.The specimens were cured during 2 months in water. They were then exposed to the same freeze-test procedure as in the main study and in the other special studies.

Companion specimens were analysed by the automatic image analyse method described in the main study.

A plot of the relation between the air content in the test specimen and the scaling after 28 cycles is shown in Fig 26. It seems as if an air content of about 4 to 5% is needed if the salt scaling resistance shall be acceptably high.

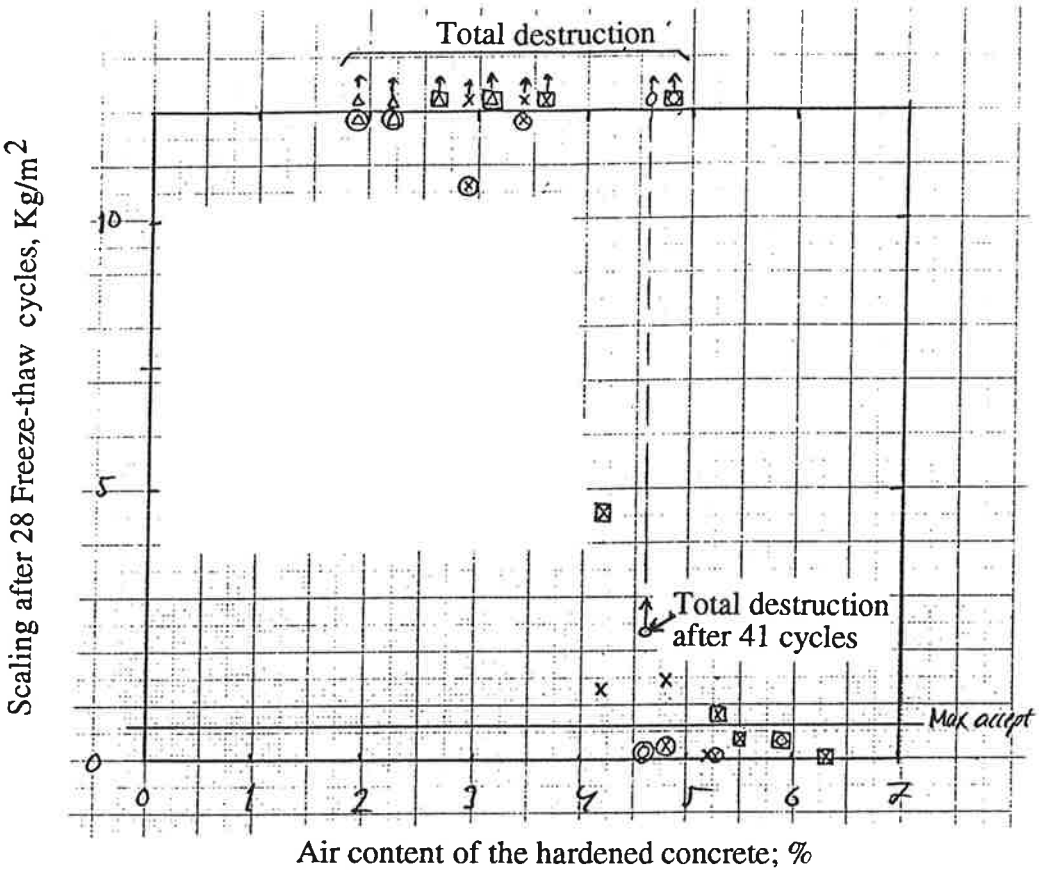

Fig 26: Special study 3: Total salt scaling after 28 freeze-thaw cycles versus the air content of the hardened concrete.

A plot of the scaling versus the fictitious spacing factor is seen in Fig 27. It is quite clear that there is a great risk of severe scaling if the spacing factor is above 0,18 mm. Below 0,18 mm there is rather small scaling although 2 concretes are above acceptable scaling despite their spacing factors are as low as 0,12 mm. There is no great difference between the two types of air-entraining agents except for the fact that it is difficult to get a low spacing factor with the agent type AW.

The critical fictitious spacing factor is:

$L_{f,CR}$ = 0,12 to 0,18 mm

Thus, as in Special study 2 some of the values are small which might depend on unstable and continuous air pore systems which was discussed above.

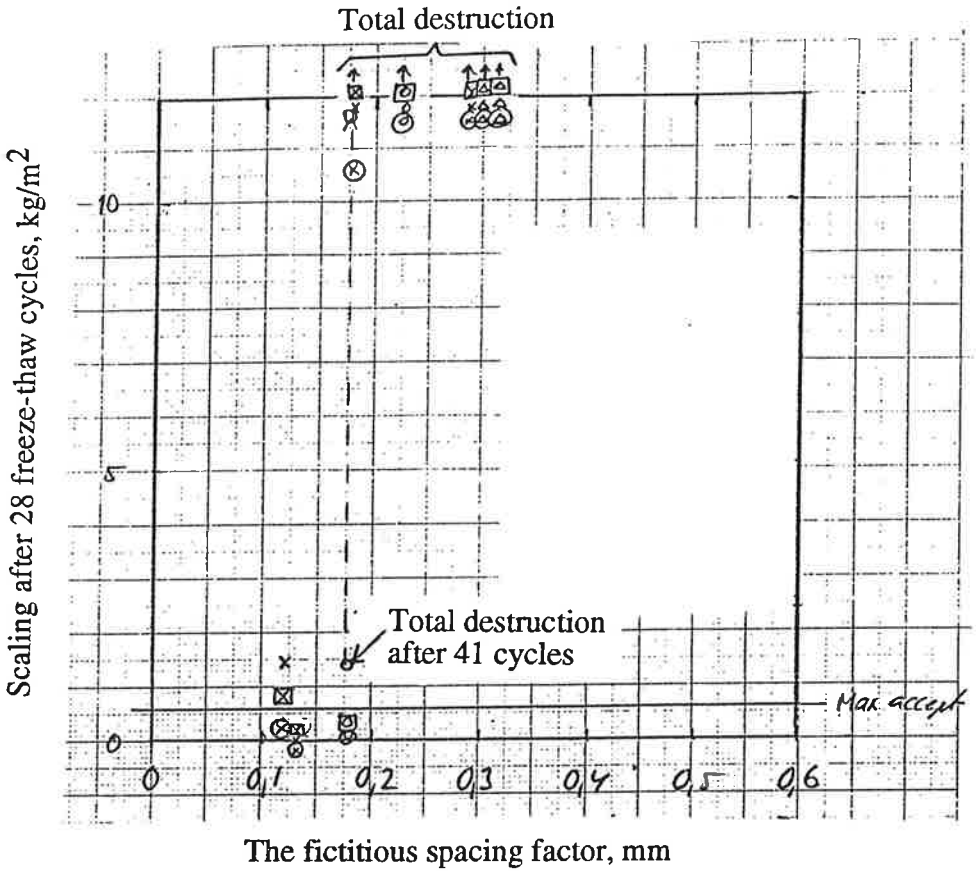

Fig 27: Special study 3: Total salt scaling after 28 freeze-thaw cycles versus the fictitious spacing factor.

3.3.5 Studies published by other authors

There are many studies reported in literature concerning the relation between the spacing factor and the salt scaling. Only one study will be shown here. Other studies will be collected and analyzed in the final version of this report.

Bonzel & Siebel /1977/ have performed a study of the weight loss of 10 cm concrete cubes freeze-thaw tested when completely immersed in 3 % NaCl-solution. The freeze-thaw cycle is similar to that used in the tests described above; i.e. 16 hours of freezing and 8 hours of thawing. The minimum temperature is however only -15°C which means that the test is a bit milder. Another difference is that the weight loss is measured as an average value of all 6 sides of the cube. In reality one gets a layering of the salt solution during the test so that the most severe scaling occurs at the bottom side while the top side is in many cases almost unharmed. The scaling values reported are therefore a bit too low. The criterion 0,6 kg/m^2 after 28 cycles used in the scaling tests discussed above corresponds to about 5 weight-% in the Bonzel & Siebel test after 100 cycles assuming scaling to be linear.

The air pore analysis was performed by the traditional manual linear traverse technique.

A plot of the weight loss after 100 cycles versus the spacing factor is shown in Fig 28. The critical fictitious spacing factor is fairly well-defined. It is :

$L_{f,CR}$ = 0,20 mm

The value is a bit higher than what was found in the previous tests. The reason might be that the lowest temperature is a bit higher. The minimum temperature has a very large influence on the scaling; c.f paragraph 3.3.1.

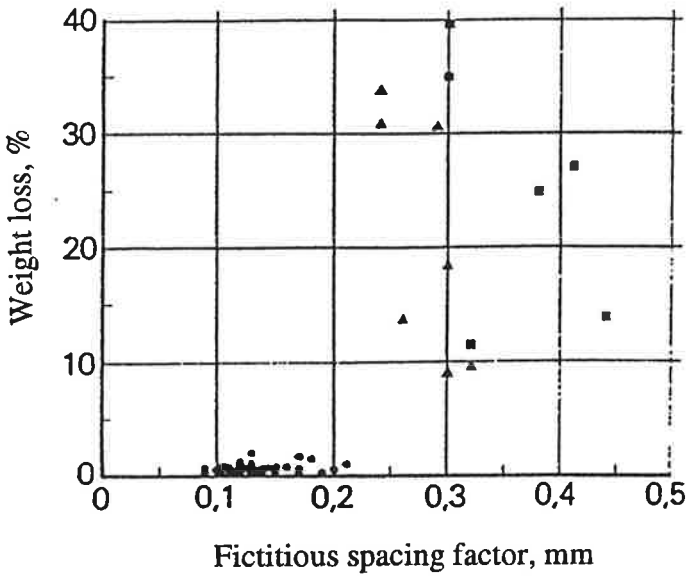

Fig 28: Relation between the weight loss after 100 freeze-thaw cycles in 3% NaCl-solution and the fictitious spacing factor. Bonzel & Siebel /1977/.

3.4 The critical fictitious spacing factor at freezing in pure water

No studies of the relation between the fictitious spacing factor and the result of a traditional freeze-thaw test in pure water have been performed by the author. Such a study is not meaningful since a large portion of the air pores become water-filled in practice. The work has instead been devoted at studies of the critical **real** spacing factor; see paragraph 4.3.

There are instead some information to be found in literature. Just one study will be presented here. A more comprehensive literature study will be presented in the final version of this report.

A study of the frost resistance of concrete was performed by Ivey & Torrans /1970/. They used the ASTM test method C666 in which the concrete is freeze-

tested in pure water. The result is expressed in terms of a "Durability Factor" (DF) which is 100% for a concrete which is not harmed at all by the 300 frost cycles involved in the test while DF=0 means that the concrete obtains so much damage that is is regarded highly undurable in a practical situation. The air pore structure of the same concretes was analyzed by the manual linear traverse method.

A plot of the durability factor versus the fictitious spacing factor is shown in Fig 29. There is a transition from a high durability factor to a low within the following interval of the fictitious spacing factor:

$L_{f,CR}$ = 0,22 to 0,25 mm

Thus, the fictitious spacing factor seems to be a bit higher when freezing takes place in pure water than when it takes place in salt water.

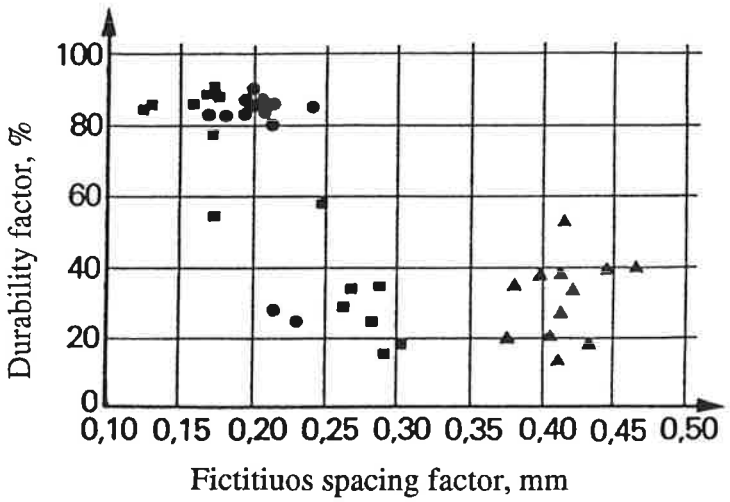

Fig 29: Relation between the durability factor of concrete tested in pure water according to ASTM C666 and the fictitious spacing factor. Ivey & Torrans /1970/.

4. The critical true spacing factor

4.1 Definition; method of determination

When the concrete is used in practice and in a real freeze-thaw test some of the air-pores become water-filled. This process of water absorption has been treated theoretically in the report Fagerlund /1993B/. This means that the real spacing factor is much bigger than the fictitious. The true critical spacing factor can be estimated if the so called critical water absorption in the air pore system is known. Then, by assuming that the water absorption starts with the smallest air pores and that a bigger pore does not start to become filled until all the smaller pores are completely filled and by knowing the size distribution of the air pores

one can calculate the critical spacing factor.
The residual "critical" air content of the partly water-filled air pore system when this is saturated critically is:

$$a_{cr} = \int_{r_{cr}}^{r_{max}} f(r) \cdot \frac{4 \cdot \pi}{3} \cdot r^3 \cdot dr \qquad (31)$$

Where

a_{cr}	the residual air pore volume (m^3)
r_{max}	the radius of the biggest air pore (m)
r_{cr}	the radius of the biggest water-filled air pore (m)
f(r)	the frequency curve of air pores
r	the pore radius (m)

The residual, "critical", total envelope area A_{cr} of the critically saturated air pore system is:

$$A_{cr} = \int_{r_{cr}}^{r_{max}} f(r) \cdot 4 \cdot \pi \cdot r^2 \cdot dr \qquad (32)$$

Then, the residual "critical" specific area α_{cr} is

$$\alpha_{cr} = A_{cr}/a_{cr} \qquad (33)$$

The critical spacing factor is calculated by eq (20) in which the total air content a and the total specific area α are exchanged for the critical air content a_{cr} and the critical specific area α_{cr}

$$L_{CR} = \{1{,}4[V_p/a_{cr}+1]^{1/3} - 1\} \cdot 3/\alpha_{cr} \qquad (34)$$

Another possibility of determining the critical true spacing factor is to freeze-thaw completely water saturated cement paste specimens in pure water or in salt water. The specimens are then broken into fragments the size of which is a measure of the critical size.

4.2 The critical true spacing factor at salt scaling

This cannot be determined by the calculation method described above because there is no good way as yet to determine "the critical degree of salt water saturation" of the air pore system. Attempts are now made to find a method of detecting this parameter. The equipment used is a combined calorimeter/dilatometer which has been built at the department; Fig 30. Dilation curves of the type shown in Fig 15 will be obtained. From them the critical saturation can be determined.

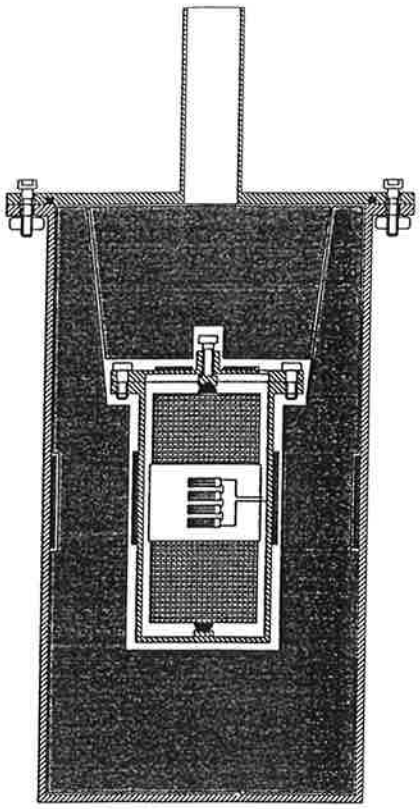

Fig 30: A combined calorimeter/dilatometer for determination of the critical degree of salt water saturation.

Some attempts have been made to determine the critical size by the other technique described above. Water cured non-airentrained cement pastes were either freeze tested directly or pre-dried and resaturated whereupon they were freeze-tested in 3% NaCl-solution. The pastes were fragmented and the fragments were passed through a sieve series. The sieve curve is a measure of the critical thickness. In fig 31 the results for the pre-dried specimens is shown. The average size is 1,8 mm for W/C-ratios above 0,5. For lower W/C-ratios the size is a bit smaller. In order to obtain the critical spacing factor one must estimate the specific surface of typical air pore structures. If a value of 15 mm^{-1} is assumed the critical spacing factor is:

L_{CR} = 0,54 mm

This value is about 3 times as big as the the critical fictitious spacing factor.

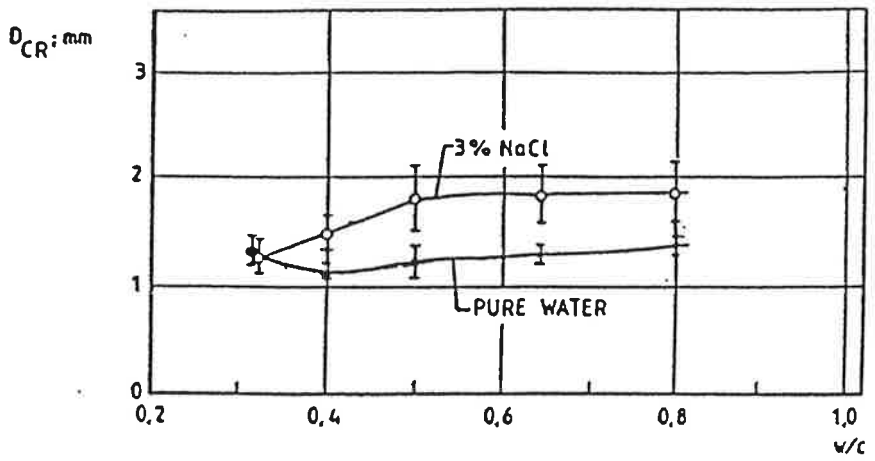

Fig 31: Direct experimental determination of the true critical thickness of pre-dried and resaturated cement pastes freeze-tested in 3% NaCl-solution or in pure water.

4.3 The critical true spacing factor at freezing in pure water

4.3.1 Main study

The critical degree of saturation and the critical air pore absorption have been determined for a large number of concretes produced within the main study described in paragraph 3.3.1. The air pore structure of the concretes was determined by automatic image analysis. On basis of these data it is possible to calculate the critical true spacing factor. This has so far only been made for one concrete. The other calculations will be published in the final version of this report.

The concrete regarded here has a W/C-ratio of 0,54 and a hardened air content of 7,1 %. The cement paste volume is 27% if no sand grains are included and 37% if sand grains smaller than 0,5 mm are included.

The chord size distribution determined is shown in Fig 32. In order to simplify the calculations the distribution is adjusted to a frequency function of the following type:

$$F(x) = \frac{a \cdot x}{b^x} \qquad (35)$$

Where

F(x)	the frequency function of chords
x	the chord length (μm)
a	constant
b	coefficient desribing the fineness of the pore system

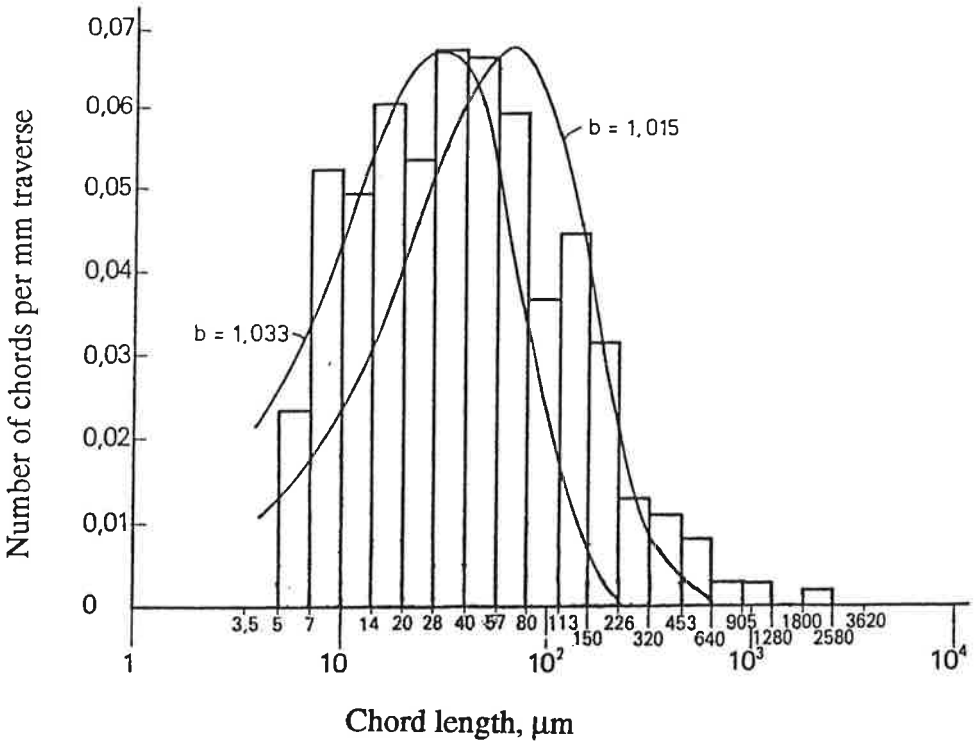

Fig 32: Main study: The chord size distribution obtained at the air pore analysis of the concrete that is treated in the text. Mathematical frequency functions -eq (35)-are also shown.

Two values of the coefficient b are used:

* Small chords, b=1,033 ($a=5{,}9\cdot10^{-3}$)
* Big chords, b=1,015 ($a=2{,}7\cdot10^{-3}$)

The two functions are plotted in Fig 32. The chord distribution can be recalculated to a sphere radius distribution F(r) by the following formula; Reid /1955/:

$$F(r) = -\frac{1}{2\cdot\pi}\cdot\frac{d}{dx}\cdot[F(x)/x] \qquad (36)$$

Insertion of eq (35) gives:

$$F(r) = \frac{a}{2\cdot\pi}\cdot\frac{\ln b}{b^r} \qquad (37)$$

The residual air content a_r and specific area α_r for different air pore absorptions can be calculated by eq (31)-(33). In Fig 33 the relation between a_r and α_r is shown for different values of the coefficient b. The dotted curve is used for the actual concrete.

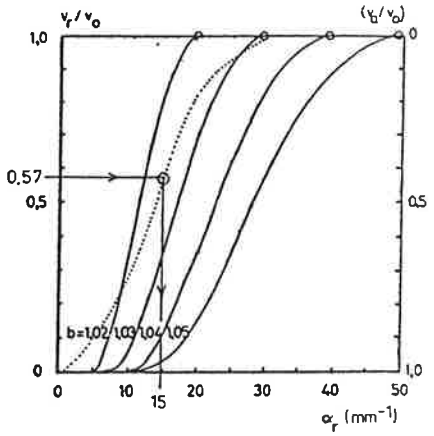

Fig 33: Relation between the residual air content and the residual specific area of pore systems that can be described by eq (37).

The result of the determination of the critical degree of saturation is shown in Fig 34. The SCR-value is 0,80. The critical degree of saturation is defined:

$$S = We/P \qquad (38)$$

Where We (m^3/m^3) is the total evaporable water content. The relation between the degree of saturation and the effective degree of saturation is; c.f. eq (7):

$$S = S_{eff}(1-k\theta) + k\theta \qquad (39)$$

The critical degree of saturation 0,80 corresponds to a residual air pore volume of 57% and, according to Fig 33, to a residual specific area of 15 mm^{-1}. The residual air content is 0,57·7,1% = 4,0%.

The critical true spacing factor can now be calculated by eq (34):

* No sand grains are included in the cement paste phase:

$$L_{CR} = \{1,4(27/4 + 1)^{1/3} - 1\}\cdot 3/15 = \mathbf{0,35\ mm}$$

* Sand grains smaller than 0,5 mm included in the cement paste phase

$$L_{CR} = \{1,4(37/4 + 1)^{1/3} - 1\}\cdot 3/15 = \mathbf{0,41\ mm}$$

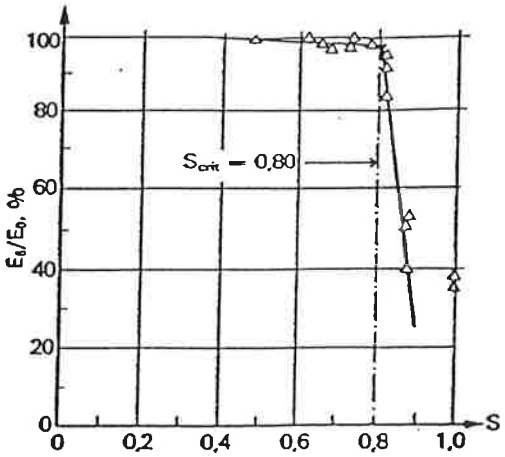

Fig 34: Main study: Experimental determination of the critical degree of saturation of the concrete that is treated in the text.

4.3.2 Special study 2; effect of the cement type

This is the same study 2 as was desribed in paragraph 3.3.3. The W/C-ratio was 0,45 in all concretes. The cement paste fraction was about 31% in all concretes.

The critical degrees of saturation are very well-defined. One example for the cement type B with the nominal air content 6% is shown in Fig 35. In Table 3 the different S_{CR}-values for all concretes are listed.

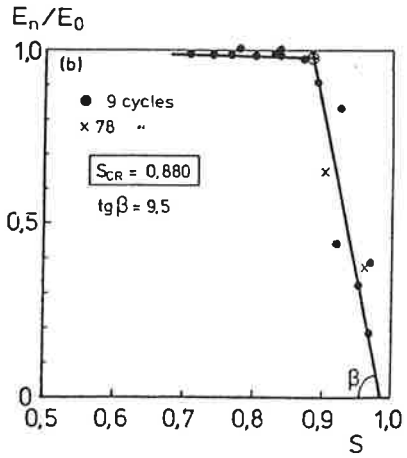

Fig 35: Special study 2: Example of the experimental determination of the critical degree of saturation. Cement type B, nominal air content 6%.

The absolute air pore distributions are shown in Fig 36. They can with fairly good precision be adjusted to a common curve:

$$F(\Phi) = a \cdot (\Phi - 0{,}015)^b \qquad (40)$$

Where

$F(\Phi)$	the distribution of pore diameters
Φ	the pore diameter (mm)
a	constant
b	coefficient describing the shape of the distribution

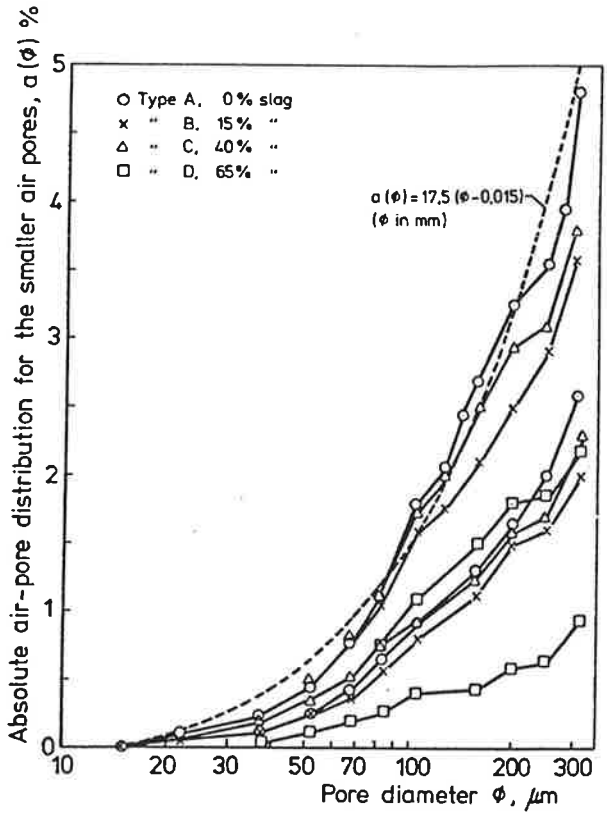

Fig 36: Special study 2: The air pore diameter distributions of all concretes.

This function is however not used. Instead the standard frequency curve eq (37) is used. The coefficient b is adjusted so that the correct specific area of the entire air pore system is obtained. Results of the calculations are shown in Table 3.

Table 3: The air pore parameter b, the critical degree of saturation S_{CR}, the critical air pore content a_{CR}, the critical specific area α_{CR} and the calculated critical true spacing factor L_{CR}.

Cement type	nominal air content (%)	b	S_{CR}	a_{CR} (%)	α_{CR} (mm^{-1})	L_{CR} (mm)
A	4,5	1,037	0,88	2,0	21	0,37
	6	1,046	0,85	2,8	25	0,27
						0,32
B	4,5	1,055	0,89	1,7	29	0,28
	6	1,045	0,88	2,1	23	0,33
						0,31
C	4,5	1,040	0,88	2,0	22	0,35
	6	1,056	0,89	1,9	28	0,28
						0,33
D	4,5	1,044	0,92	1,3	22	0,42
	6	1,051	0,91	1,5	25	0,35
						0,39
				Mean value		**0,33**
				Stand. dev.		0,05

The critical spacing factors are also plotted in Fig 37. The value is not quite constant which might depend on the fact that a standard air pore distribution curve was used and not the real curve. There is also a slight tendency of increasing value with increasing slag content. However, on basis of the results in this special study and the result presented under the main study it seems reasonable to assume that the critical true spacing factor for freezing in pure water is:

L_{CR} = 0,30 to 0,35 mm

No sand grains are then supposed to be included in the cement paste fraction.

4.3.3 Direct determination of the critical size

In paragraph 4.2 were presented the results from a direct determination of the critical size by freezing of saturated cement pastes in salt water. At the same time a parallell test was made in which the pre-dried and resaturated specimens were frozen in pure water. The result of the sieve analysis of the fragments is shown in Fig 31. The critical thickness is almost independent of the W/C-ratio. The average size is 1,2 mm. This corresponds to a certain spacing factor the size

of which is somewhat depending of the size of the air pore. If this is supposed to correspond to a specific area of 15 mm^{-1} the following critical spacing factor is obtained:

L_{CR} = 0,40 mm

This is of the same order of size as that calculated from the critical absorption.

Literature

Bager D. Sellevold E: The effect of the moisture history on the ice formation in hardened cement paste. In "Frost resistance of concrete. Nordic Research Seminar 23 Oct. 1982. CBI, Report Ra 2.83, Stockholm, 1983. (In Danish.)

Beskow G: Soil frost and frost heave with regard to roads and railways. Sveriges Geologiska Undersökningar, Annual book 26, Stockholm, 1935 (In Swedish.)

Bigg EK: The supercooling of water. Proc. Physical Society. B66, London, 1953.

Bonzel J: Siebel E: Neuere Untersuchungen über den Frost-Tausaltz-Widerstand von Beton. Beton Heft 4,5 and 6, 1977.

Collins AR: The destruction of concrete by frost. J. Inst. Civil Eng., Paper No 5412, London, 1944.

Defay R,Prigogine I, Everett DH: Surface tension and adsorption. Longmans, London, 1966.

Fagerlund G: Non-freezable water contents of porous building materials. Div. of Building Materials, Lund Inst. of Technology, Report 42, 1974.

Fagerlund G, Modéer M: Unpublished calorimeter experiments. Div. of Building Materials, Lund Inst. of Technology, 1974.

Fagerlund G: Equations for calculating the mean free distance between aggregate particles or air pores in concrete. CBI Research Fo 8:77, Stockholm 1977.

Fagerlund G: Frost resistance of concrete with porous aggregate, CBI, Research Fo 2:78, Stockholm, 1978.

Fagerlund G: Influence of slag on the frost resistance of concrete- a theoretical analysis. CBI, Research Fo 1:80, Stockholm, 1980.

Fagerlund G: The critical size in connection with freezing of porous materials. Cementa, Rapport CMT 86039, Danderyd, Sweden, 1986.

Fagerlund G: Studies of the scaling, the water uptake and the dilation of specimens exposed to freezing and thawing in NaCl-solutions. In "Freeze-thaw and de-icing resistance of concrete". Div. Building Materials, Lund Institute of Technology, Report TVBM-3048, 1992.

Fagerlund G: Frost attack- description of the mechanisms. Div. of Building Materials, Lund Inst. of Technology, Report TVBM-7056, 1993.(in Swedish.)

Fagerlund G: The long time water absorption in the air pore structure of concrete. Div. of Building Materials, Lund Inst. of Technology, Contribution to the BRITE/EURAM project

BREU-CT92-0591, Lund, 1993.

Ivey DL, Torrans PH: Air void systems in ready mixed concrete. J . of Materials, Nr 5, 1970.

Johansson L: Damage of concrete balconies. CBI, Research Fo 3:76, Stockholm, 1976.

Jung F: über die Frostbeständigkeit des jungen Betons. Zement-Kalk-Gips, Nr 3, 1967.

Larson TD, Cady PD: Identification of frost susceptible particles ion concrete aggregates. National Cooperative Highway Research Program, Report 66, 1969.

Lindmark S: Influence on the salt scaling of variations in the salt concentration, the salt distribution and the freeze-thaw cycle. Div. of Building Materials, Lund Institute of Technology, Report TVBM-7055, 1993.

Malmström K: The importance of cement composition on the salt-frost resistance of concrete. Swedish National Testing Institute, SP Report 1990:07, Borås, Sweden, 1990.

Mielenz RC, Wolkodoff VE, Backstrom JE, Flack HL, Burrows RW: Origin, evolution and effects of the air void system in concrete. Part 1 Entrained air in unhardened concrete. J. ACI, Vol 30, 1958.

Penner E: Pressures developed in a porous granular system as a result of ice segregation. Highway Res. Board, Special Report Nr 40, 1958.

Philleo RE: A method for analyzing void distribution in air-entrained concrete. Portland Cement Ass. Tentative Paper, Chicago, 1955.

Pistilli MF: Air void parameters developed by air entraining admixtures as influenced by soluble alkalies from fly ash or portland cement. J. ACI, May-June, 1983.

Powers TC, Brownyard TL: Physical properties of cement paste. Res. Labs. Cem. Ass. Bull. 22, Chicago, 1948.

Powers TC: The air requirement of frost resistant concrete. Proc. Highway Res. Board, No29, 1949.

Powers TC, Helmuth RA: Theory of volume changes in hardened portland cement paste during freezing, Proc. Highway Res. Board, No 32., 1953.

Powers TC: Resistance of concrete to frost at early ages. Proc. RILEM Symp. "Winter concreting", Copenhagen, 1956.

Powers TC: Prevention of frost damage to green concrete. Bull. RILEM No 14, 1962.

Reid WP: Distribution of sizes of spheres in a solid from a study of the slices of the solid. J. of Mathematics and Physics, Cambridge, Mass. 34, 1955.

Sellevold E, Bager D, Klitgaard-Jensen E, Knudsen T: Silica fume cement pastes. In "Condensed silica fume in concrete", Div Building Materials, Norwegian Inst. of Technology, Report BML 86.610, Trondheim 1982.

Timoshenko S, Goodier JN: Theory of elasticity, McGraw-Hill, New York, 1951.

Vuorinen J: On determination of effective degree of saturation of concrete. Manuscript, Concrete and soil Laboratory, Imatran Voima, Oulo, Finland, 1973.